2455-5

Joint ICTP-TWAS Workshop on Portable X-ray Analytical Instruments for Cultural Heritage

29 April - 3 May, 2013

Lecture NoteBasic principles of X-ray Computed Tomography

Diego Dreossi
Elettra, Trieste
Italy

Strada Costiera, 11 - 34151 - Trieste - Italy • Tel. +39 0402240111 • Fax. +39 040224163 • sci_info@ictp.it • www.ictp.it
ICTP is governed by UNESCO, IAEA, and Italy, and it is a UNESCO Category 1 Institute

Workshop on Portable X-ray Analytical Instruments for Cultural Heritage
ICTP, Trieste, 29 april - 3 may, 2013

Basic principles of X-ray Computed Tomography

Diego Dreossi

Sincrotrone Trieste, S.S. 14 km 163.5

AREA Science Park 34012 Basovizza (TS), Italy

Acknowledgements

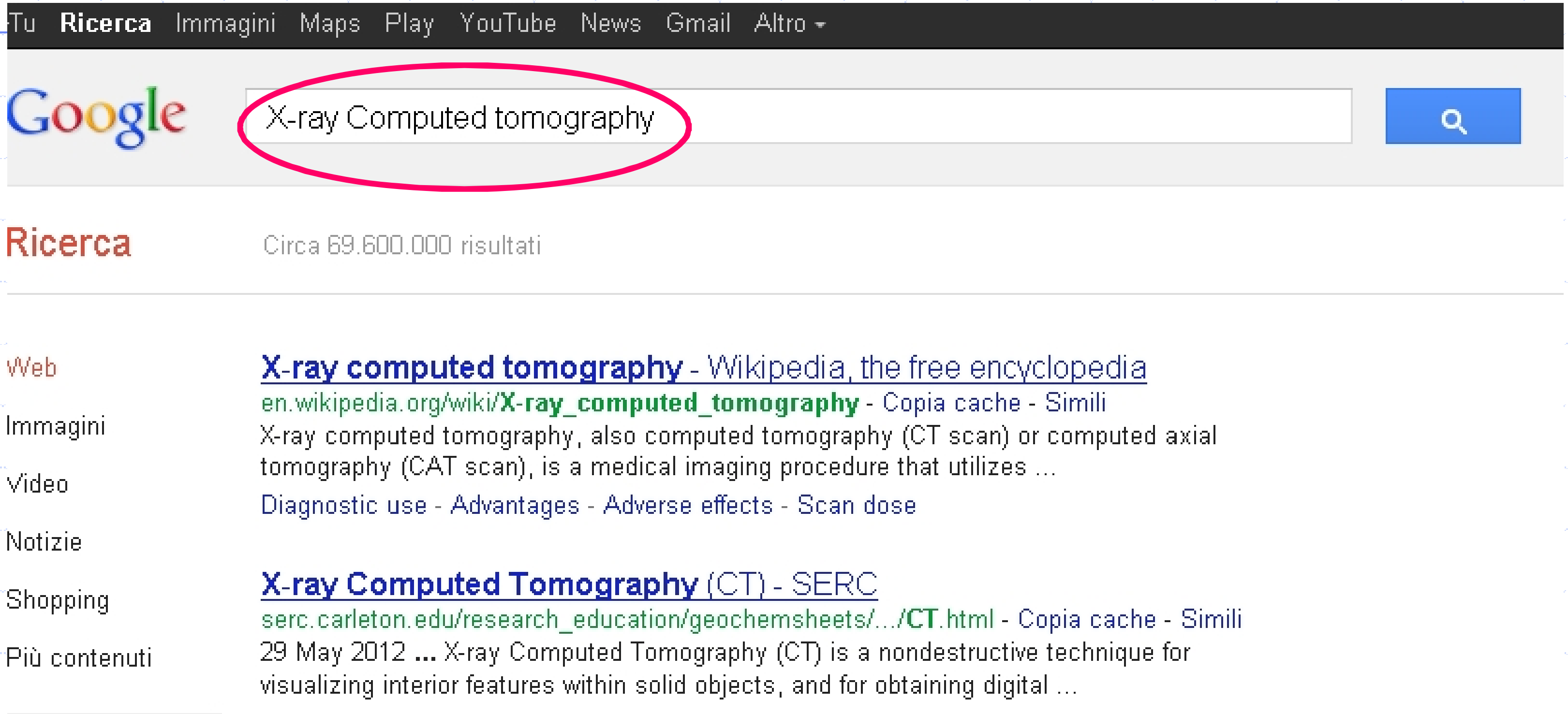

Thanks to the big CT community for all the information and material available on the web!

Tomography

The word *tomography* is derived from the Greek τομως ("part" or "section") and γραφειν ("to write")

Object

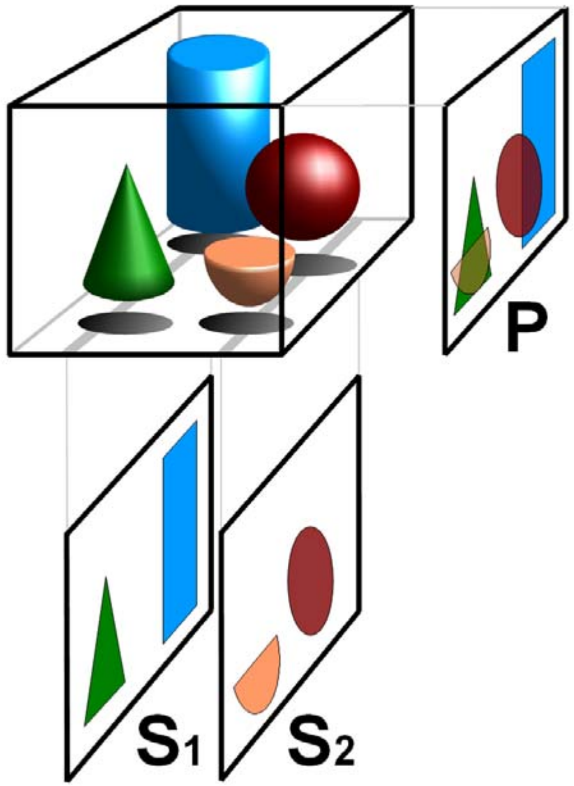

Projected image

Sections

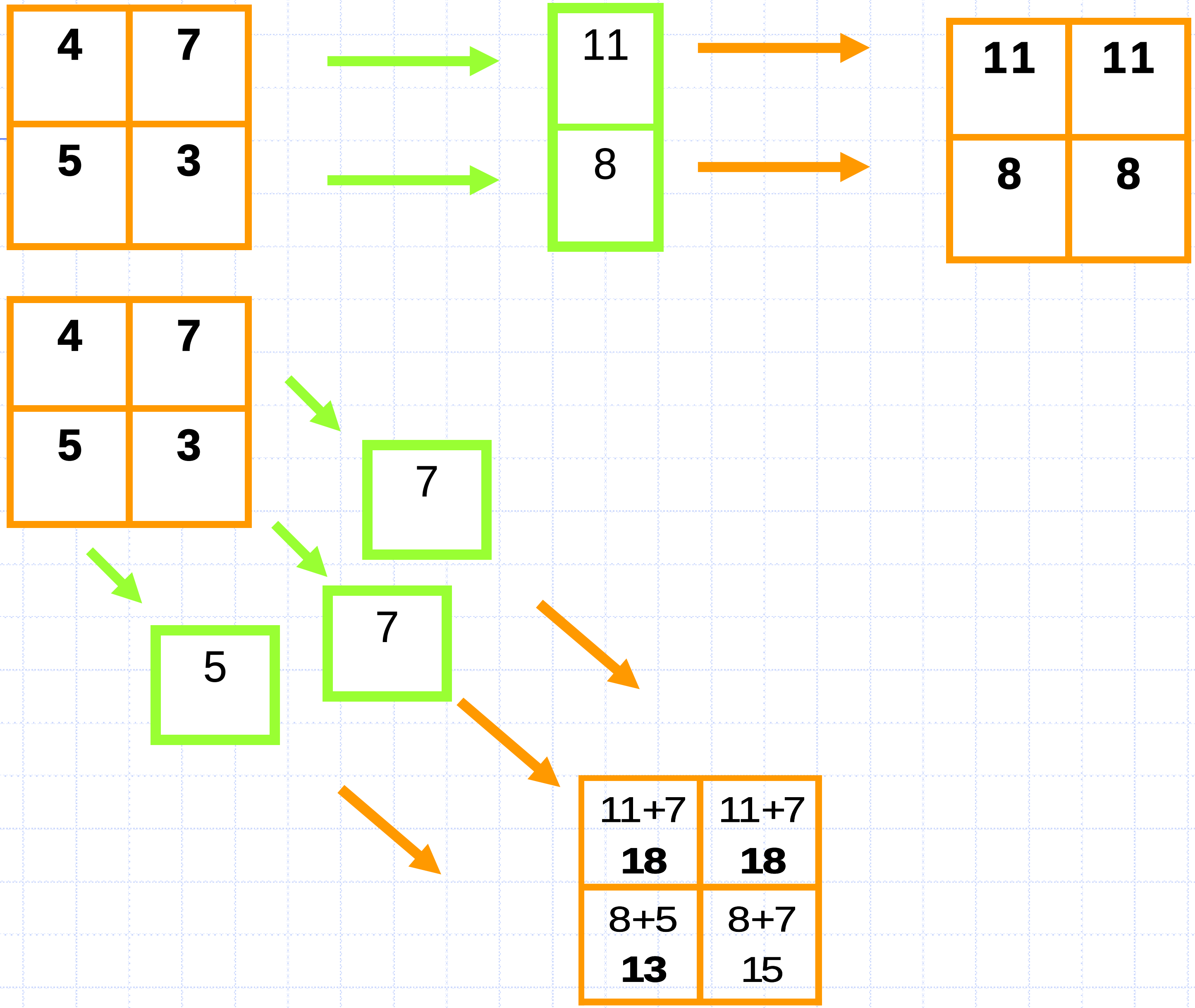

4
7
5
3
11
8
11
11
8
8
4
7
5
3
7
7
5
11+7
18
11+7
18
8+5
13
8+7
15

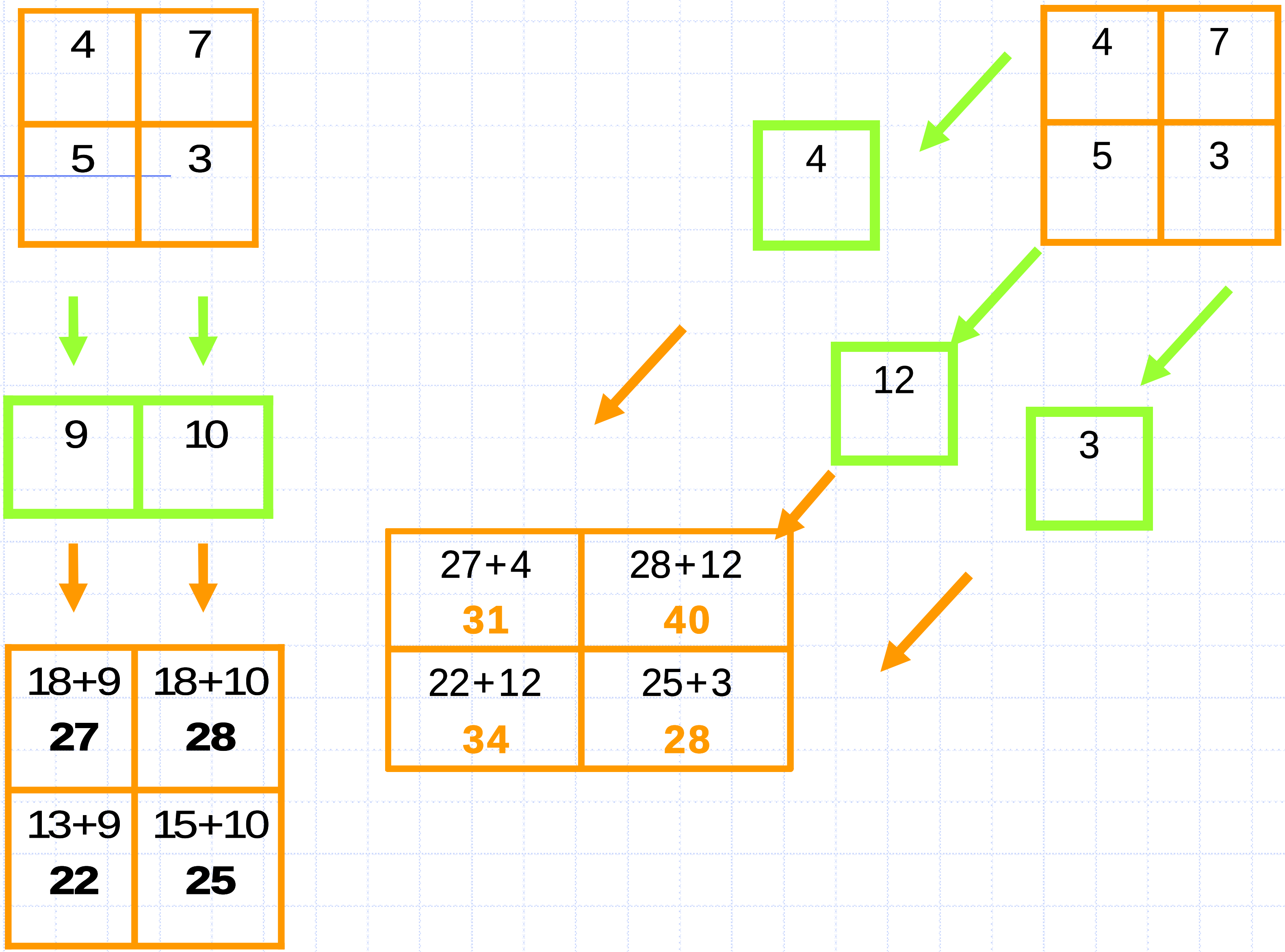
4
7
5
3
9
10
18+9
27
18+10
28
13+9
22
15+10
25
4
7
5
3
4
12
3
27+4
31
28+12
40
22+12
34
25+3
28

31	40
34	28

-19

12	21
15	9

/3

4	7
5	3


Worth1000.com

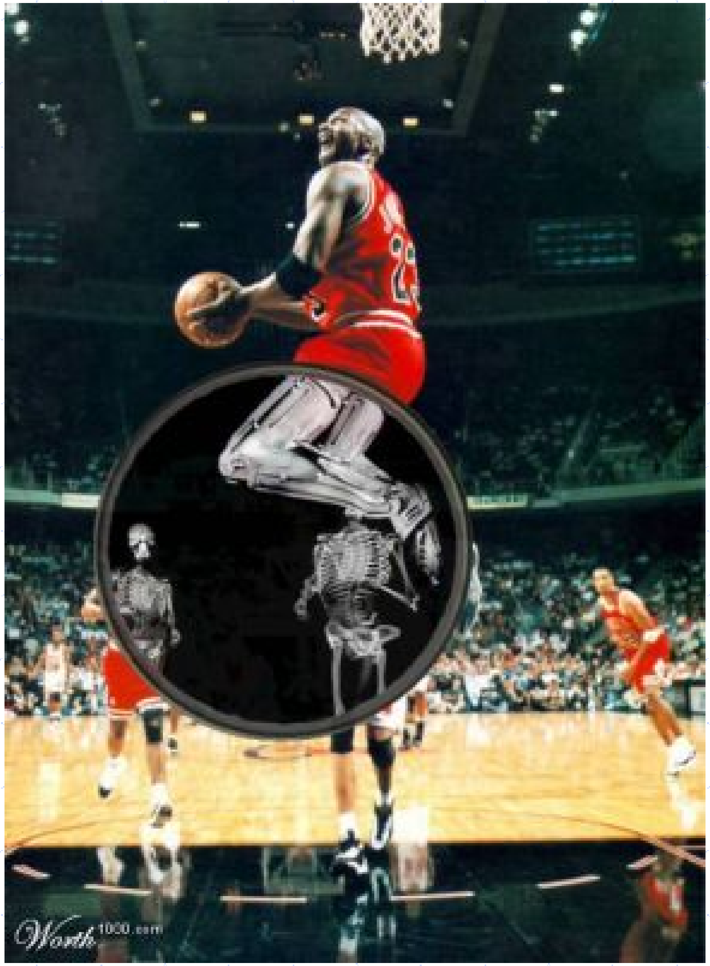
Worth1000.com


Worth1000.com


Worth1000.com


Worth1000.com

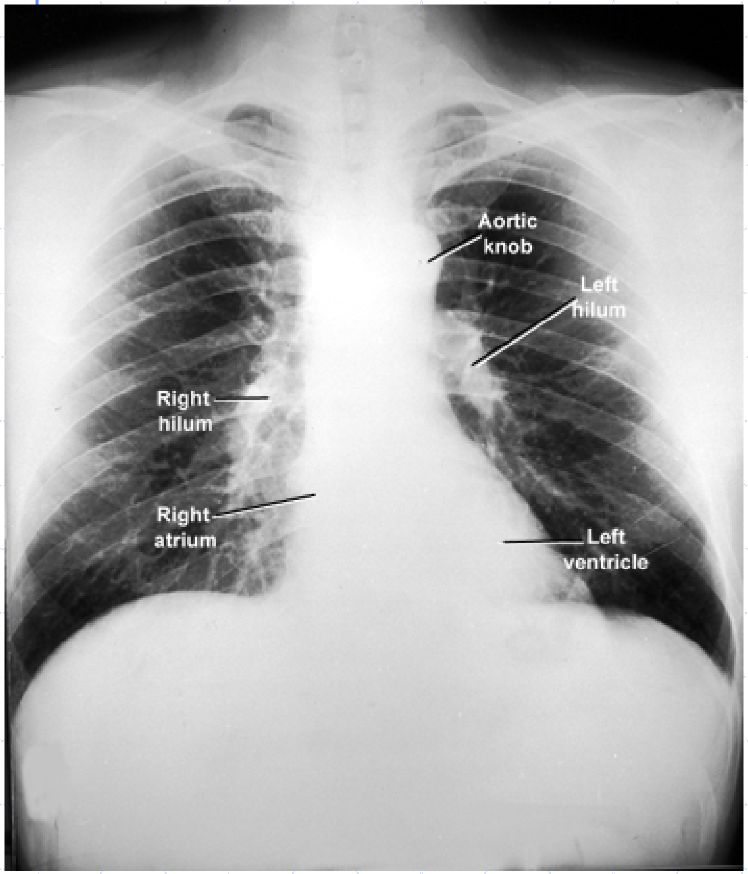
Aortic knob
Left hilum
Right hilum
Right atrium
Left ventricle

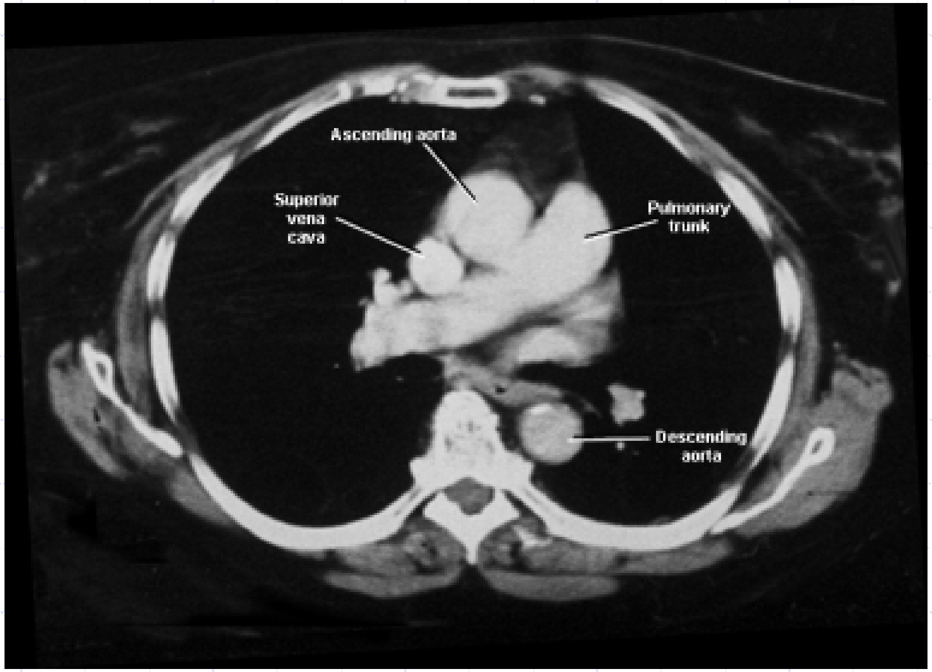
Ascending aorta
Superior vena cava
Pulmonary trunk
Descending aorta

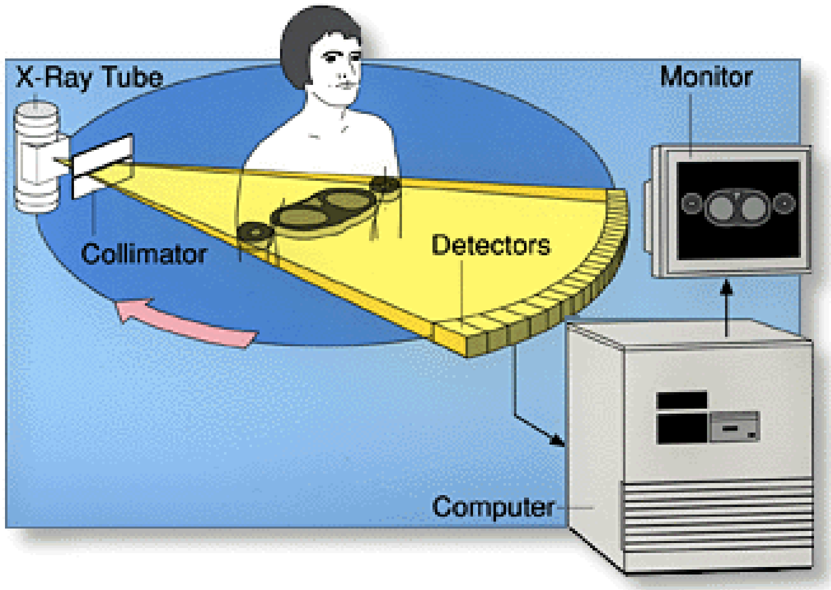
X-Ray Tube
Monitor
Collimator
Detectors
Computer

Basic interactions

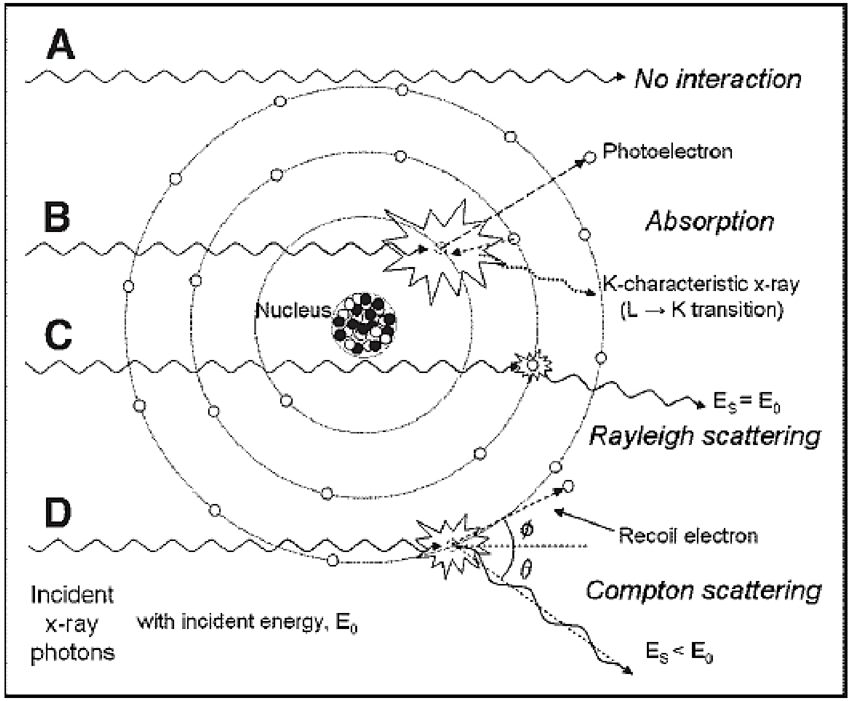

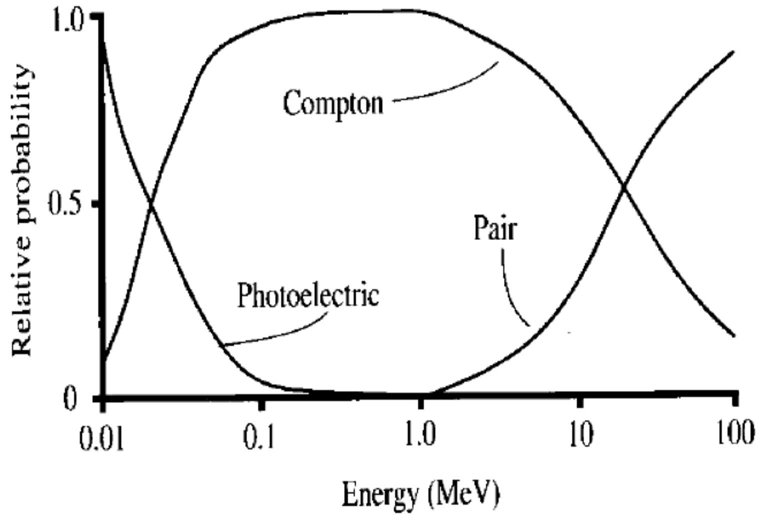

TABLE 1
Summary of X-Ray–γ-Ray Interactions

Process	Interaction	Z, E, ρ effects	Comments
Photoelectric absorption	Photon energy > electron binding energy, photon absorbed, electron ejected from shell with kinetic energy equal to $E_{photon} - E_{BE}$	$\tau \propto Z^3/E^3$	Atom is ionized; high imparted energy; characteristic radiation is be released; generates maximum differential signal
Rayleigh scattering	Photon interacts with bound atomic electron without ionization; photon is released in different direction without loss of energy	$\sigma_R \propto 1/E^{1.2}$	No energy absorption occurs; photons mainly scattered in forward direction
Compton scattering	Photon interacts with "free" electron, ionizes atom; energy of incident photon shared with scattered photon and recoil electron	$\sigma \propto \rho$ $\sigma \propto E^{0*}$ $\sigma \propto 1/E^{\dagger}$	Displaced electron energy is absorbed locally; interaction produces attenuation and partial absorption
Pair production	Photon energy > 1.02 MeV interacts with nucleus and conversion of energy to e^-–e^+ charged particles; e^+ subsequently annihilates into two 511-keV photons	$\pi \propto (E - 1.02\ \text{MeV}) \times Z$	Probability of interaction increases with increasing energy, unlike other processes

*Within diagnostic x-ray energy range of 10–100 keV.
†At energies > 100 keV.
E_{BE} = electronic binding energy.

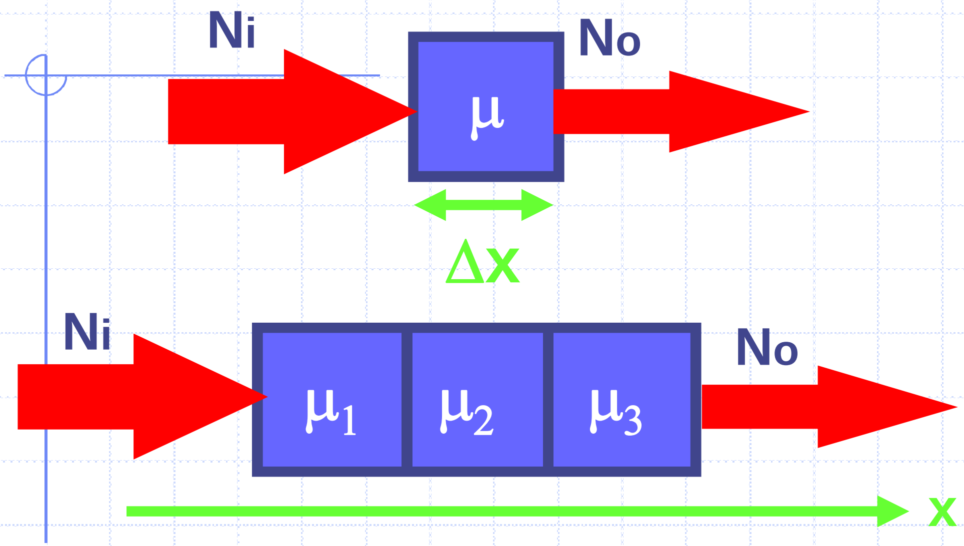

$$N_o = N_i e^{-\mu \Delta x}$$

$$N_o = N_i e^{-(\mu_1 + \mu_2 + \mu_3)\Delta x}$$

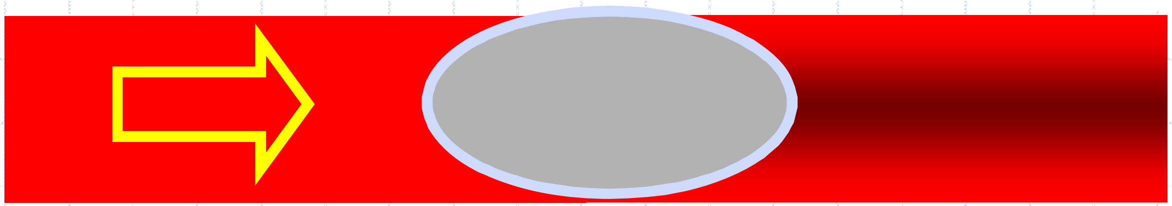

Attenuation

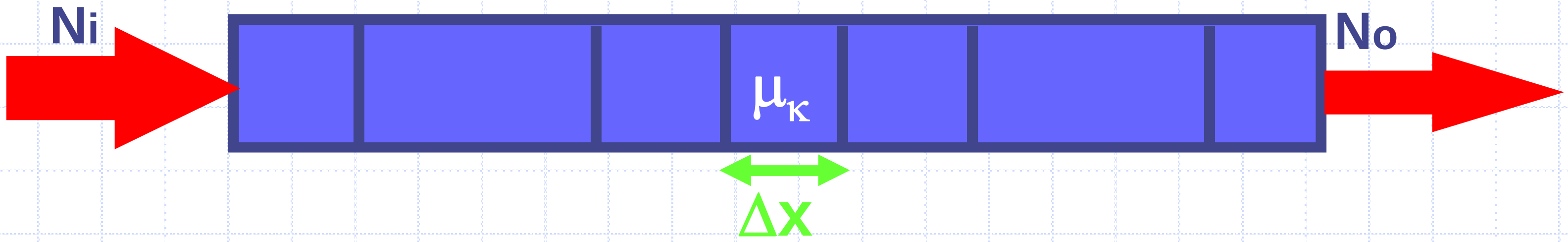

$$N_o = N_i e^{-\sum_k \mu_k \Delta x}$$

$$\sum_k \mu_k \Delta x = \ln \frac{N_i}{N_o}$$

$$\int_{-\infty}^{\infty} \mu(x)\,dx = \ln \frac{N_i}{N_o}$$

Line integral

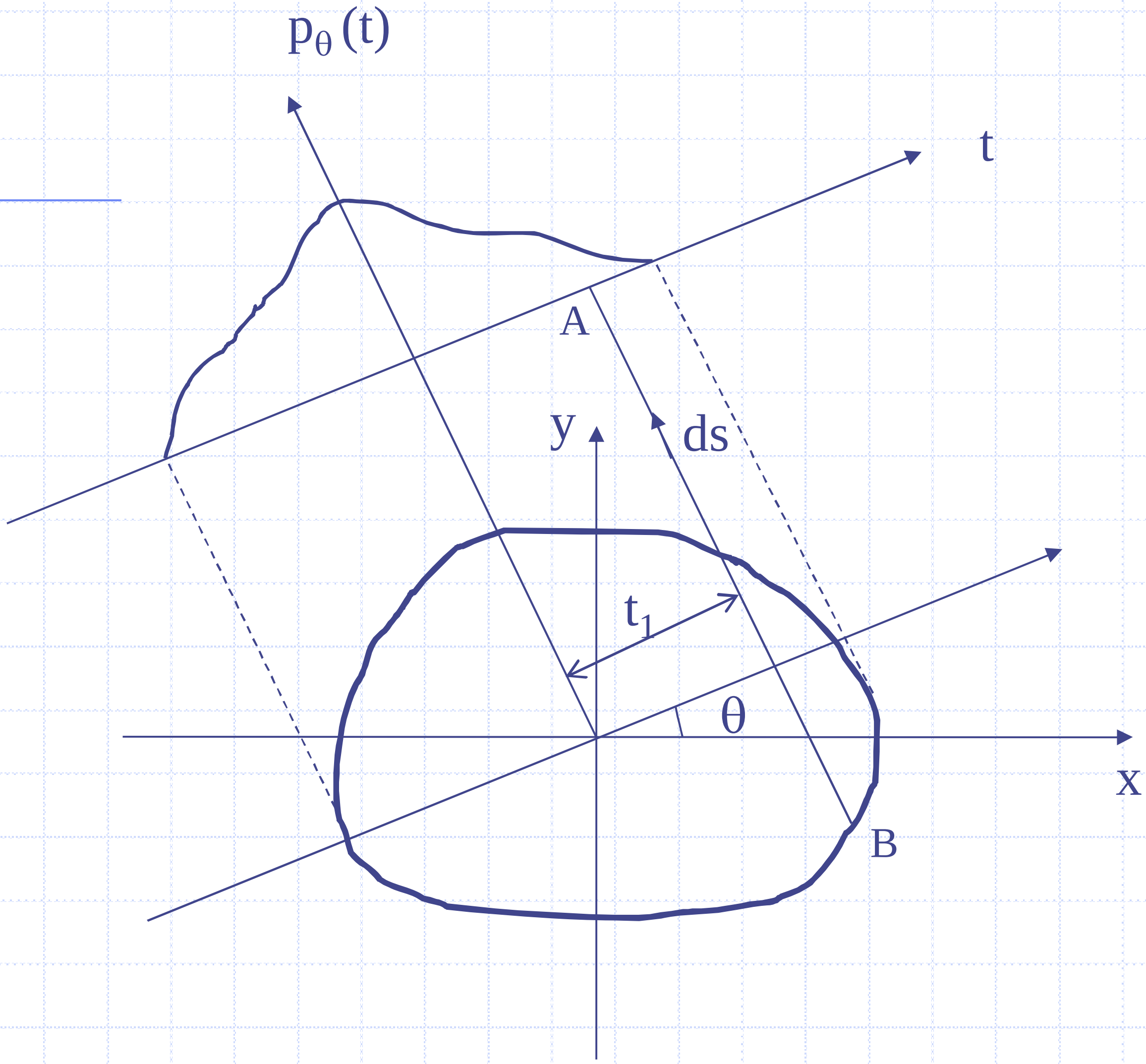

The projection function is also determined by the angle of view θ .

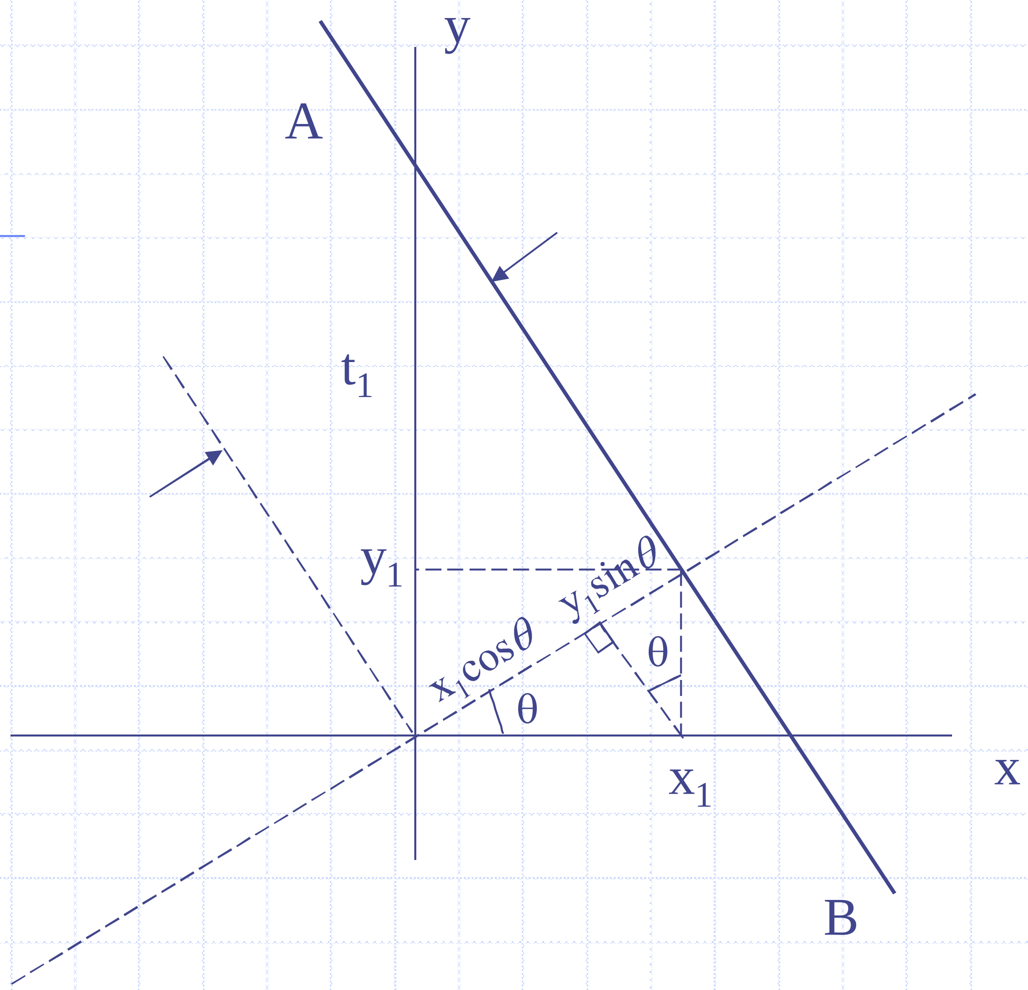

The equation of line AB is $x\cos\theta + y\sin\theta = t$

The projection function can be written as

$$p_\theta(t) = \int_{(\theta,t)\ line} \mu(x,y)\, ds$$

$$p_\theta(t) = \int_{-\infty}^{\infty}\int_{\infty}^{\infty} \mu(x,y)\,\delta(x\cos\theta + y\sin\theta - t)\, dxdy$$

$p_\theta(t)$ is known as the *Radon Transform* of the function $\mu(x,y)$.

A projection is formed by combining a set of line integrals.
The simplest projection is a collection of parallel ray integrals as given by $p_\theta(t)$ for a constant θ. This is known as *parallel projection*.

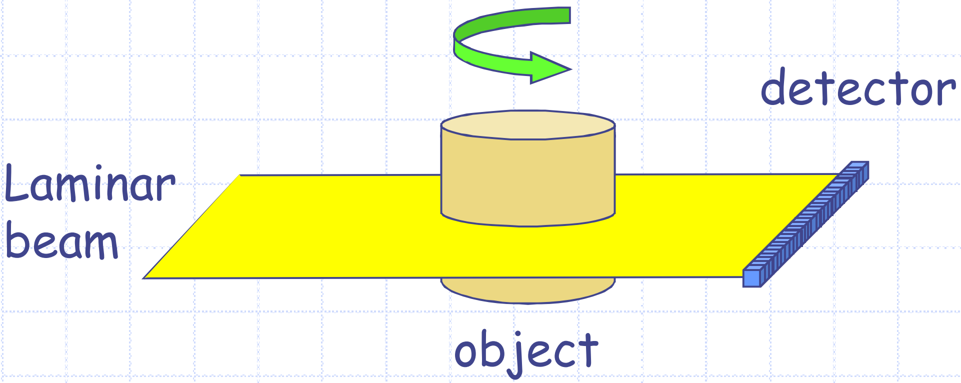

Image reconstruction algorithms are derived to construct $\mu(x,y)$ from $p_\theta(t)$.

Classification of Algorithms

Backprojection

Fourier Domain Approach

Filtered Backprojection

Iterative Methods

Algebraic Reconstruction Technique (ART)

Iterative Least Squares

Simultaneous Iterative Reconstruction Technique (SIRT)

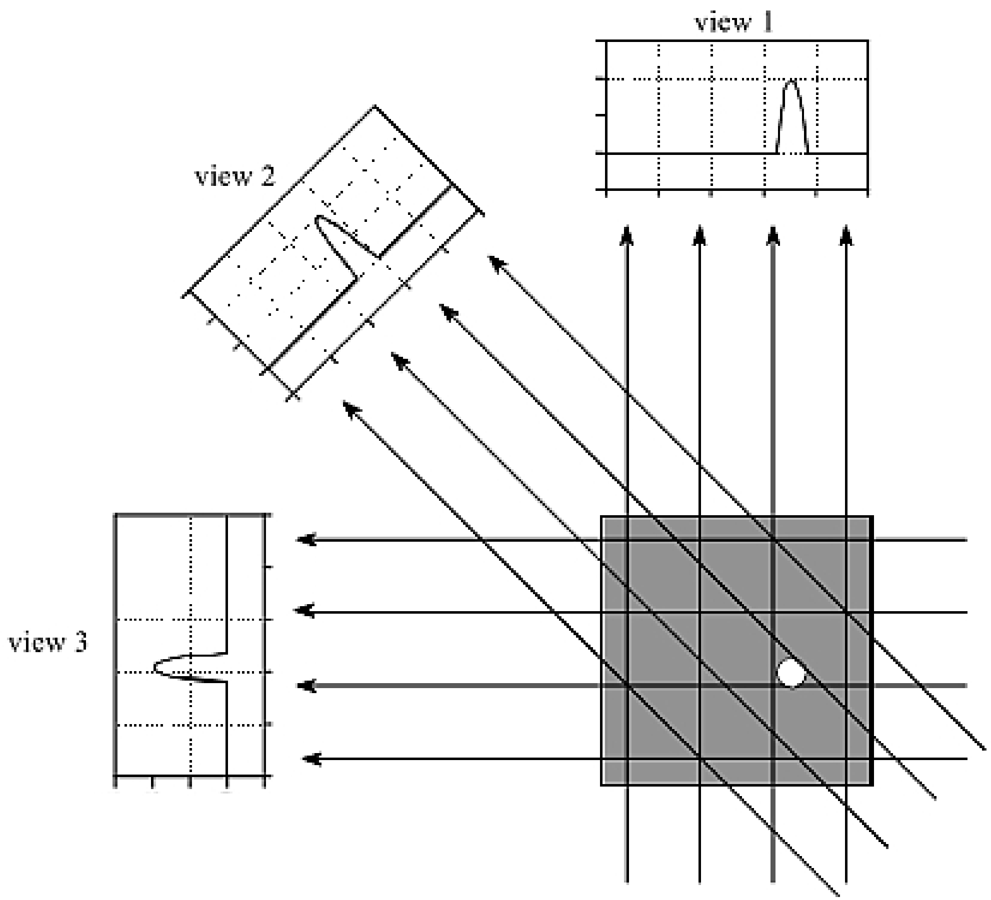
view 1
view 2
view 3

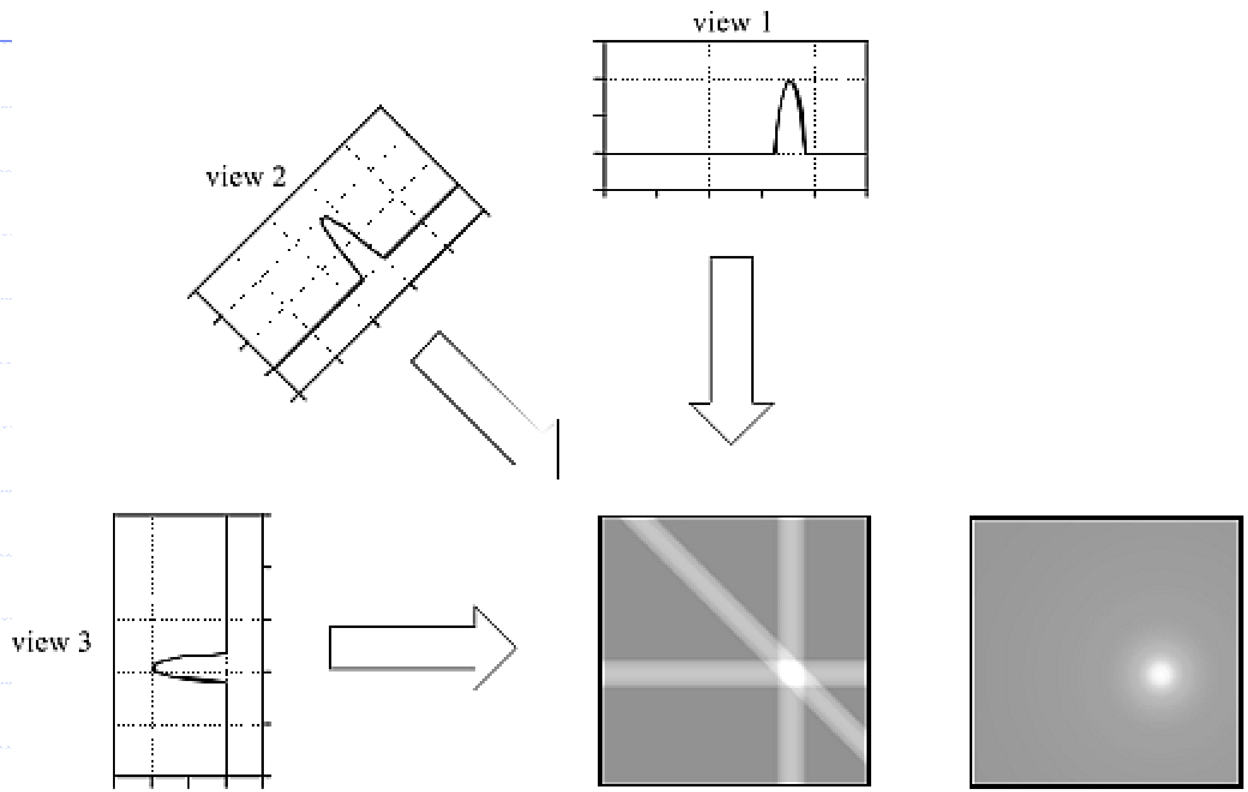

a. Using 3 views

b. Using many views

The above given process can be expressed mathematically. The reconstructed back-projection image $b_\theta(x,y)$ at a particular view θ is :

$$b_\theta(x,y) = \int p_\theta(t)\,\delta(x\cos\theta + y\sin\theta - t)\,dt$$

Adding up the images at all angles (0-π)

$$f_b(x,y) = \int_0^\pi b_\theta(x,y)\,d\theta$$

$$= \int_0^\pi \int_{-\infty}^{\infty} p_\theta(t)\,\delta(x\cos\theta + y\sin\theta - t)\,dt\,d\theta$$

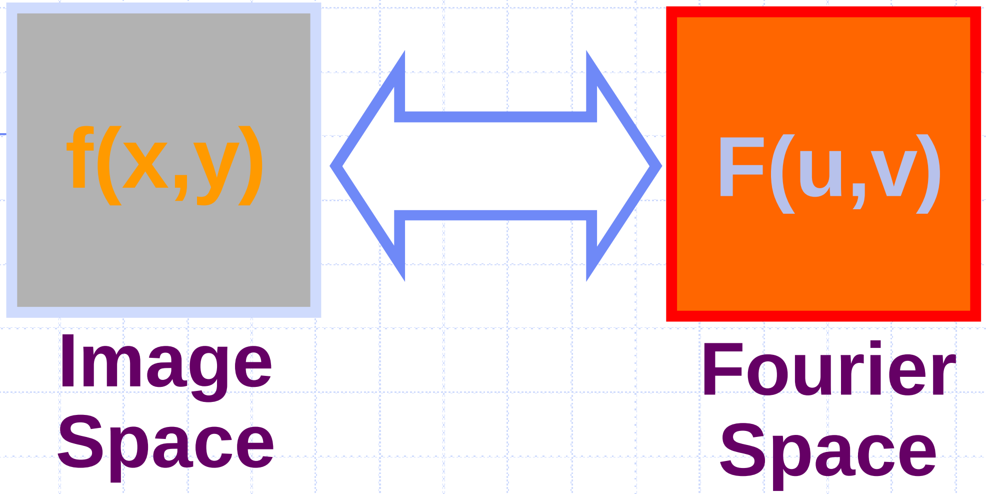

$$F(u,v) = F\left[f(x,y)\right] = \int_{-\infty}^{\infty}\int_{-\infty}^{\infty} f(x,y)e^{-j2\pi(ux+vy)}dxdy$$

$$f(x,y) = F^{-1}\left[F(u,v)\right] = \int_{-\infty}^{\infty}\int_{-\infty}^{\infty} F(u,v)e^{j2\pi(ux+vy)}dudv$$

The Fourier transform of a parallel projection of an image $f(x,y)$ taken at angle θ gives a slice of the 2D transform, $F(u,v)$, subtending an angle θ with the u-axis. In other words, the Fourier Transform of $P_\theta(t)$ gives the values of $F(u,v)$ along line BB in Figure 6.

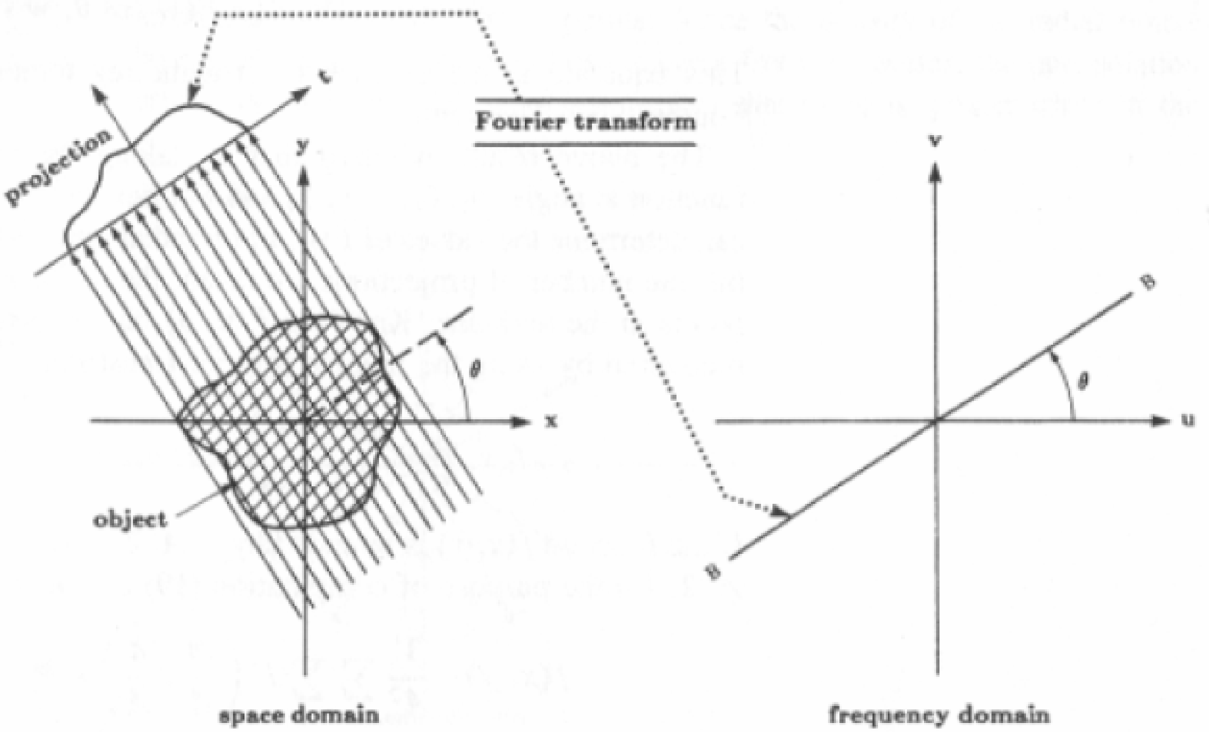

Figure 6 - Example of Fourier Slice Theorem. Fourier Transform of a projection at angle θ fills in a straight line at angle θ in the 2D Fourier Transform of the image. [4].

- Thus the Fourier Transform of a projection at angle β forms a line in the 2-D Fourier plane at this angle.
- After filling the entire $F(\rho,\beta)$ plane with the transforms of the projections at all angles, the object can be reconstructed using 2-D Inverse Fourier Transform

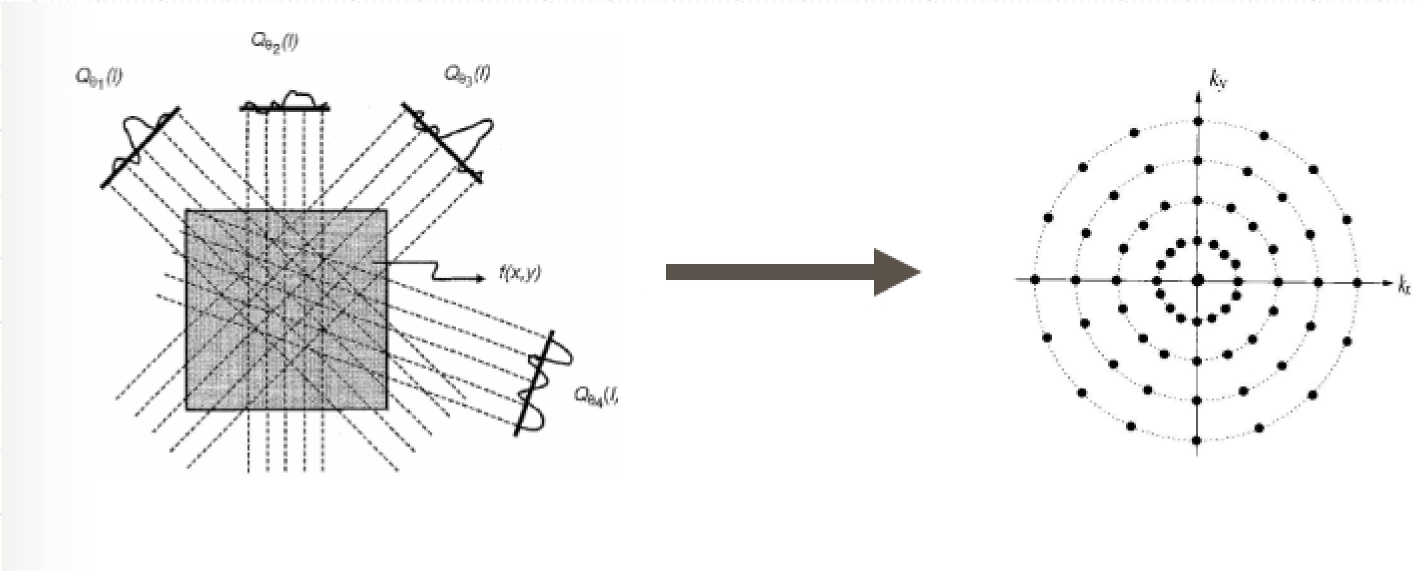

Convolution Back-projection Algorithm

The back-projected function can rewritten in space domain as follows:

$$F_1^{-1}\left\{F_1\left\{p_\theta(t)\right\}\cdot|\rho|\right\} = p_\theta(t) * \underbrace{F_1^{-1}\left\{|\rho|\right\}}_{c(t)}$$

Thus, instead of filtering in the frequency domain,
p_θ(t) can be convolved with a function c (t) and then back-projected.

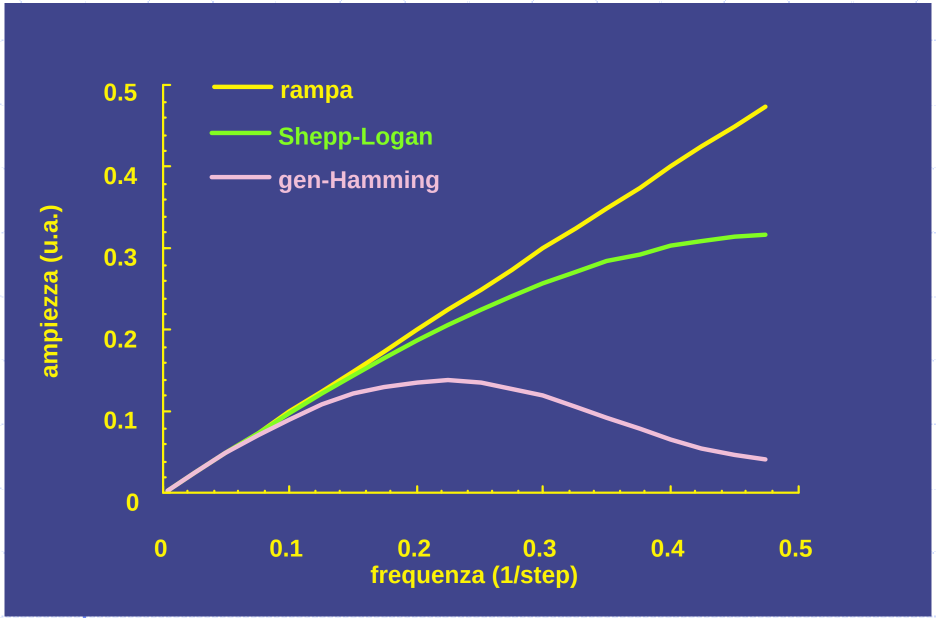

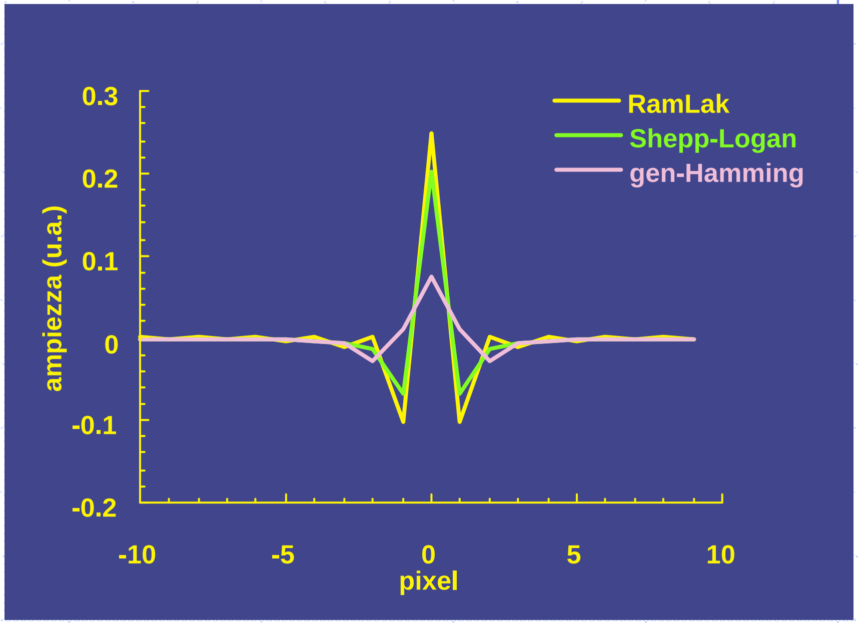

- Ramp filter (RamLak): enhancement of high frequencies → noise
- Gen-Hamming, Shepp-Logan: enhancement of intermediate frequencies
- Convolution theorem → convolution in the direct space as an alternative to multiplication in the Fourier space

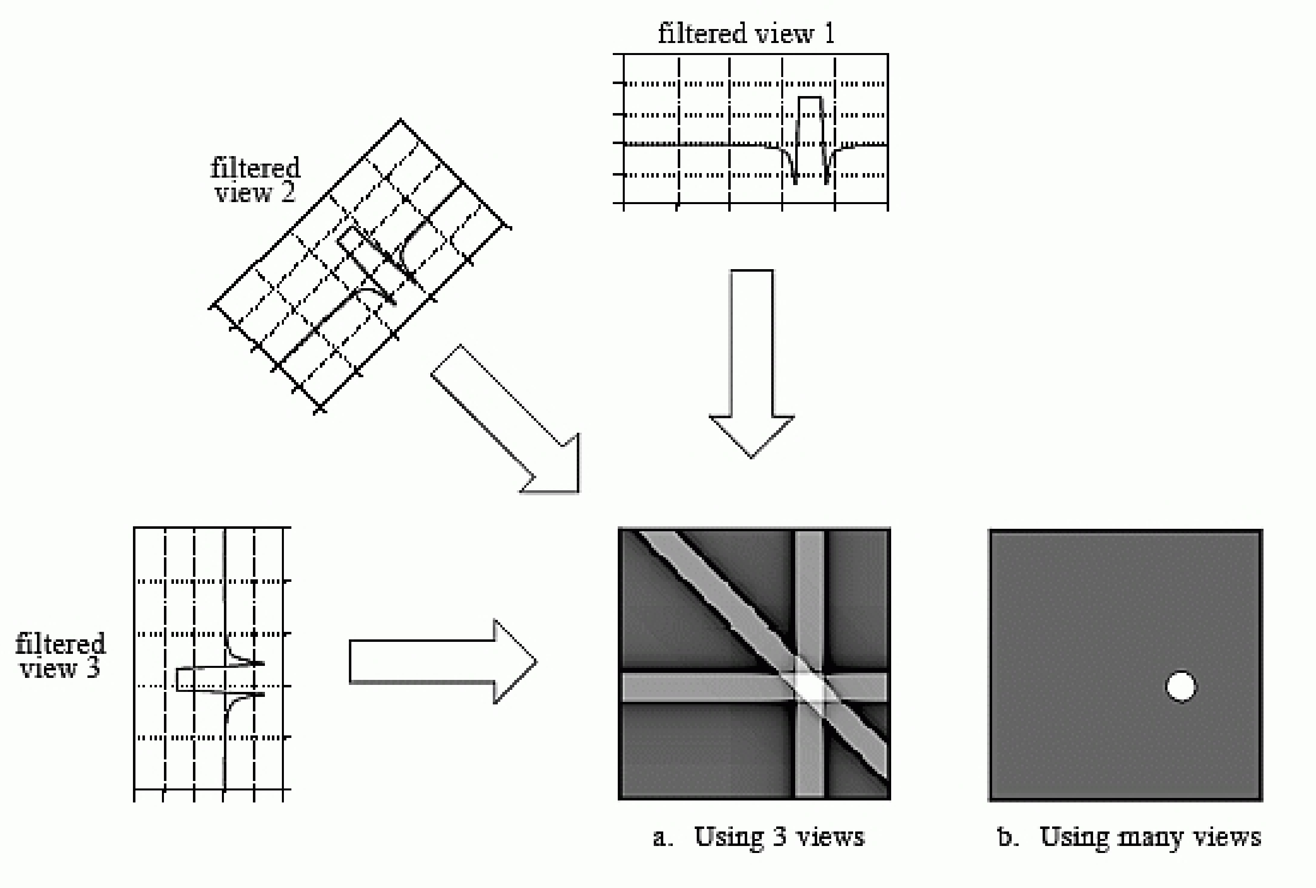
filtered view 1
filtered view 2
filtered view 3
a. Using 3 views
b. Using many views

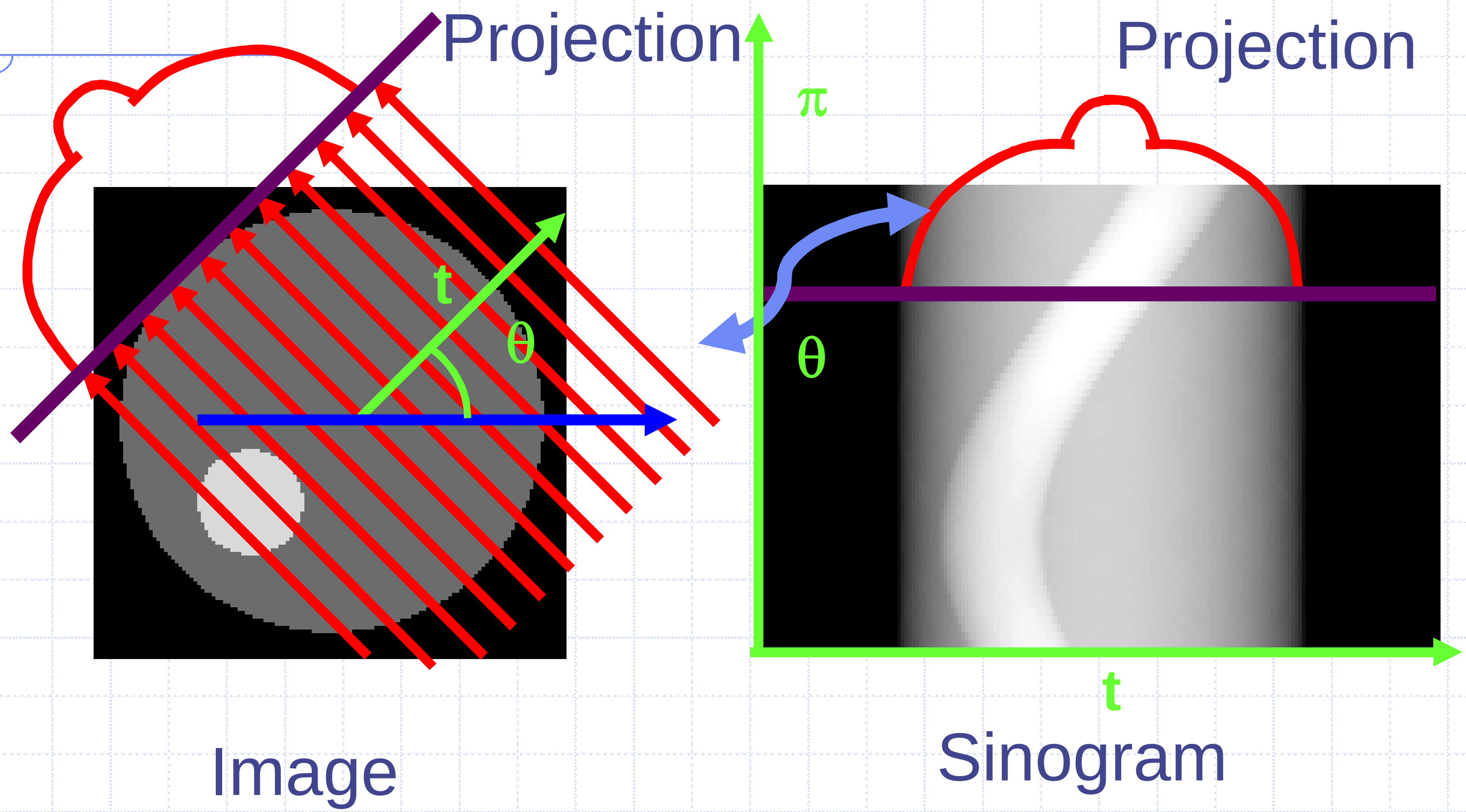

Projection
t
θ
π
θ
Projection
t
Image
Sinogram

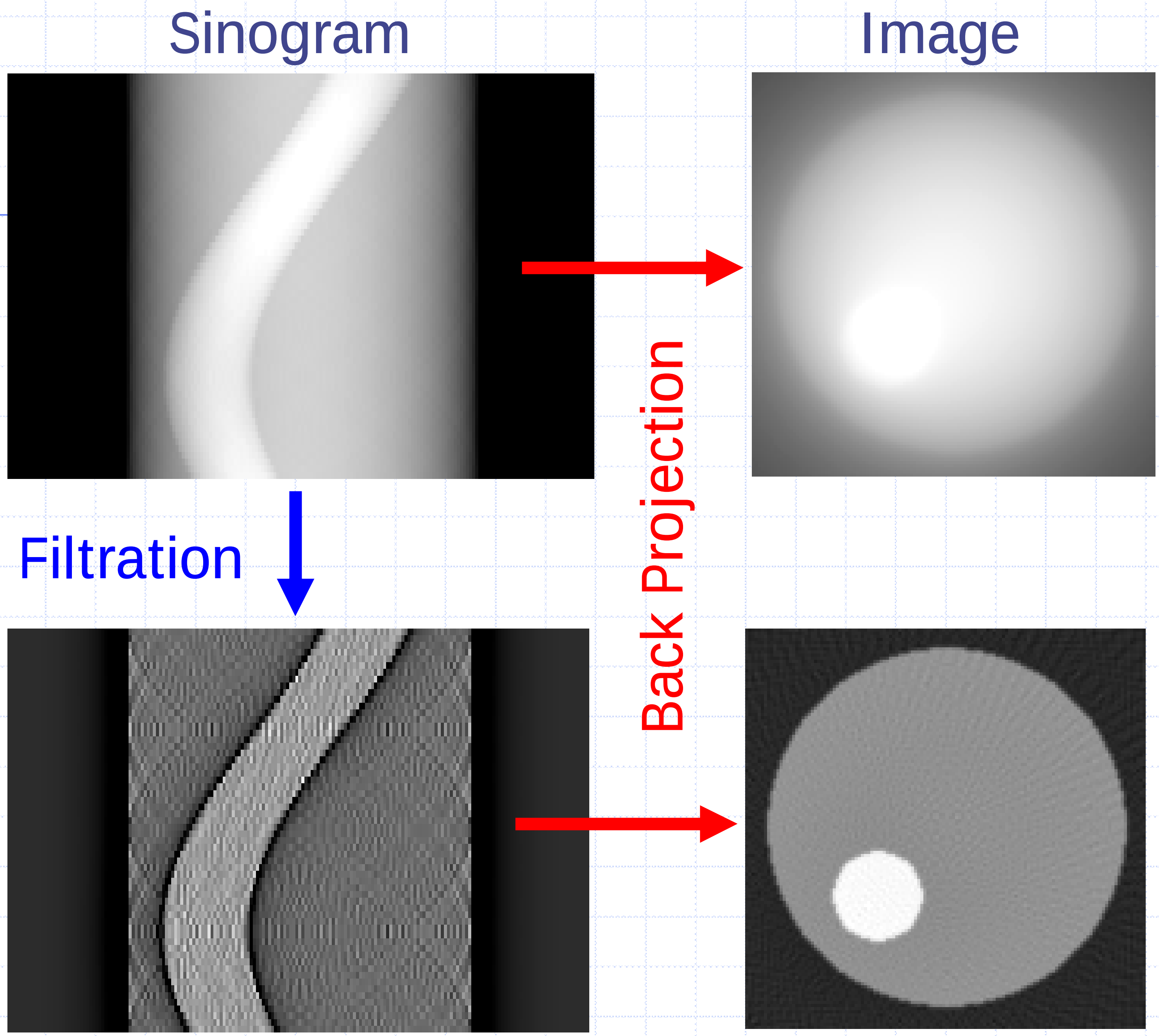
Sinogram
Image
Filtration
Back Projection

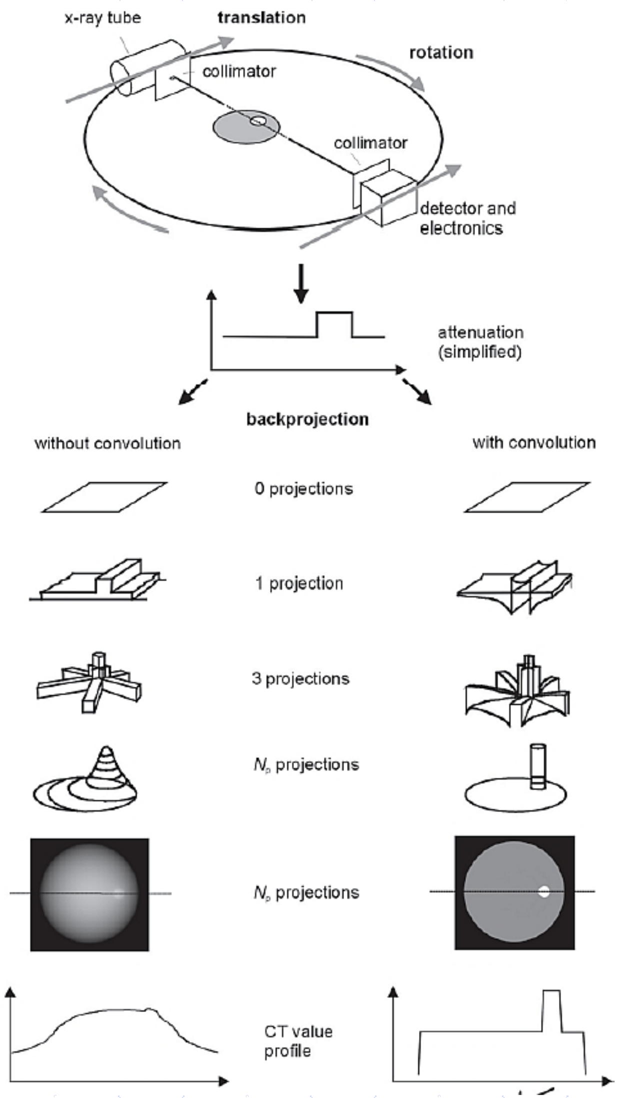
x-ray tube
translation
rotation
collimator
collimator
detector and
electronics
attenuation
(simplified)
backprojection
without convolution
with convolution
0 projections
1 projection
3 projections
N_p projections
N_p projections
CT value
profile

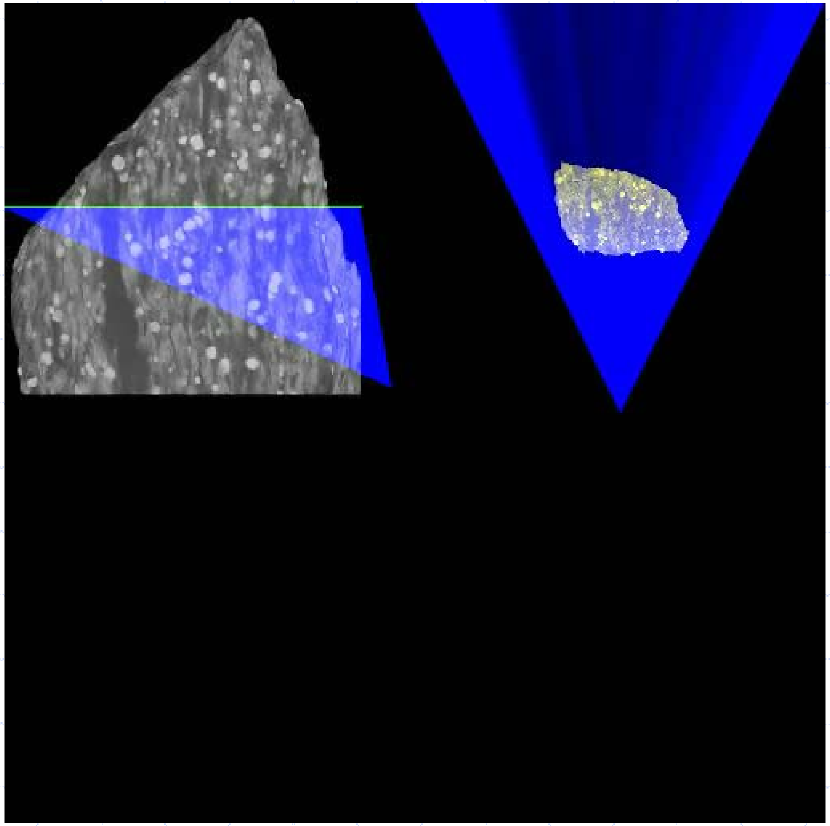

Reconstruction in frequency domain

- Interpolation can be used in the frequency domain to re-grid the radial sampling to uniform sampling
- Inverse DFT can then be efficiently used to compute the image

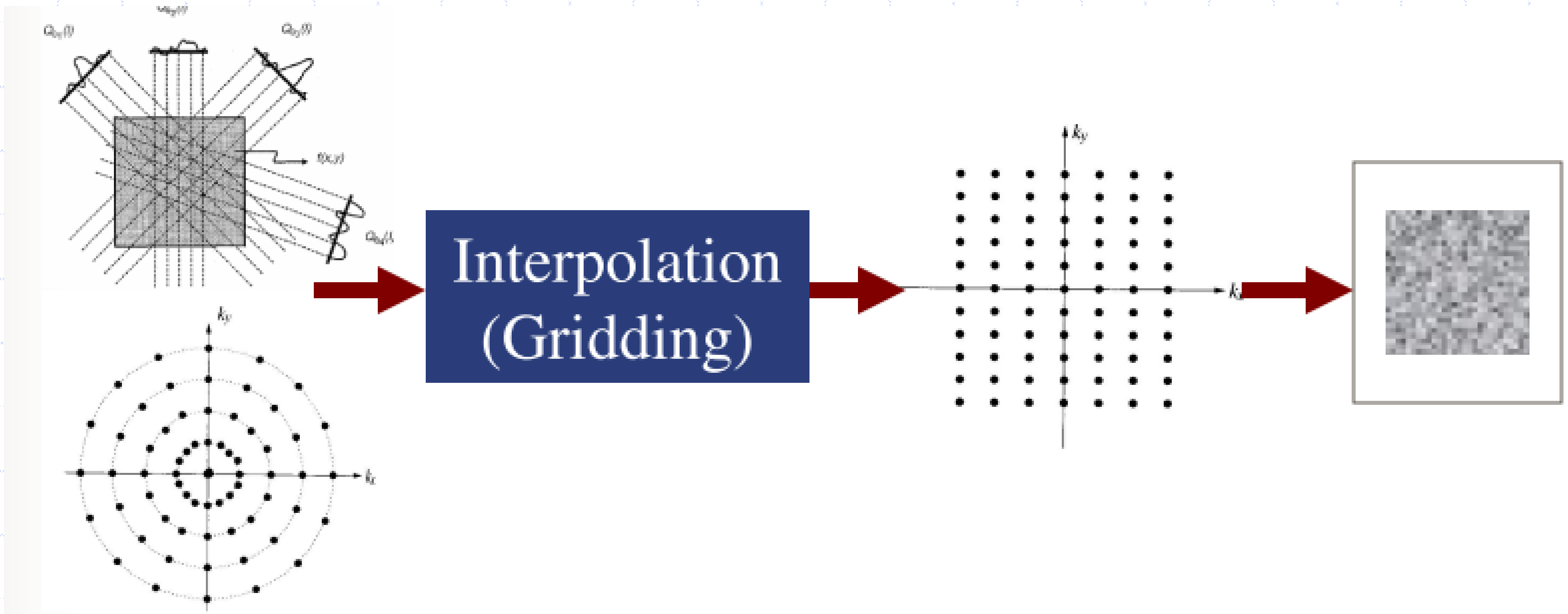

ART

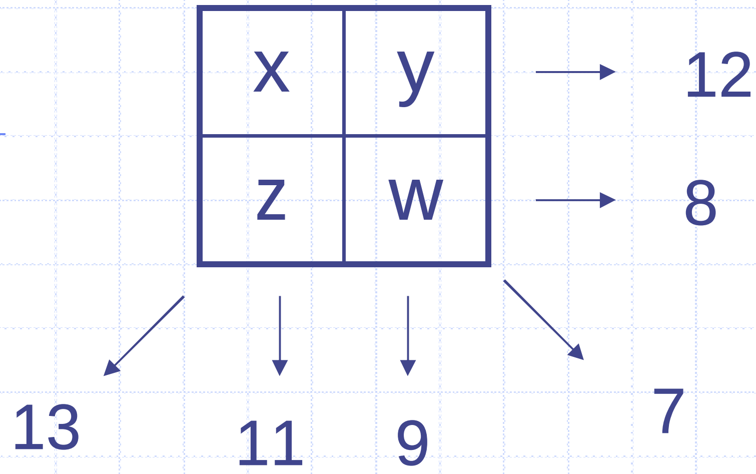

$$\begin{bmatrix} 1 & 1 & 0 & 0 \\ 0 & 0 & 1 & 1 \\ 1 & 0 & 1 & 0 \\ 0 & 1 & 0 & 1 \\ 1 & 0 & 0 & 1 \\ 0 & 1 & 1 & 0 \end{bmatrix} \begin{bmatrix} w \\ x \\ y \\ z \end{bmatrix} = \begin{bmatrix} 12 \\ 8 \\ 11 \\ 9 \\ 7 \\ 13 \end{bmatrix}$$

First generation

- EMI Mark I (Hounsfield), “pencil beam” or parallel-beam scanner
- 180° - 240° rotation angle, angular step ~1 °
- Scan time 5 min, reconstruction time 20 min
- Resolution: 80 x 80 pixels (ea. 3 x 3 mm^2),
- Slice thickness 13 mm

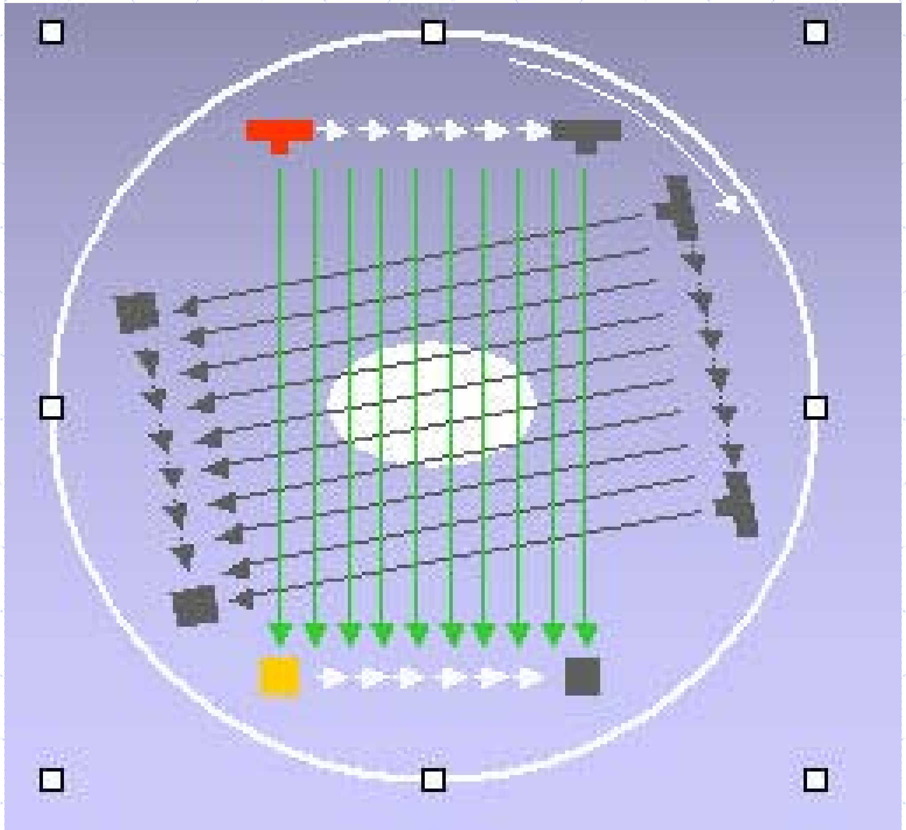

Second generation

- Hybrid system: Fan beam + linear array (~30 elements)
- traslation and rotation
- total scan time ~30 s
- more complex agorithms (“fan” geometry)

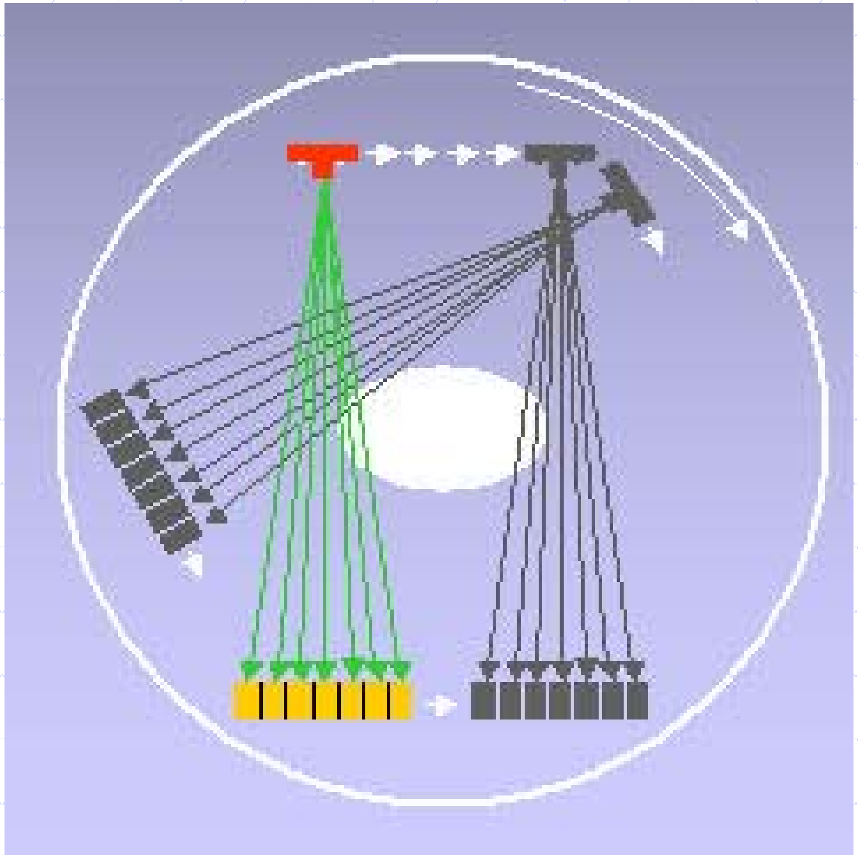

Third generation

- the fan beam is covering all the sample
- 500-700 elements (ionizating chambers or scintillators)
- No traslations
- total scan time ~ seconds
- reconstruction time ~ seconds

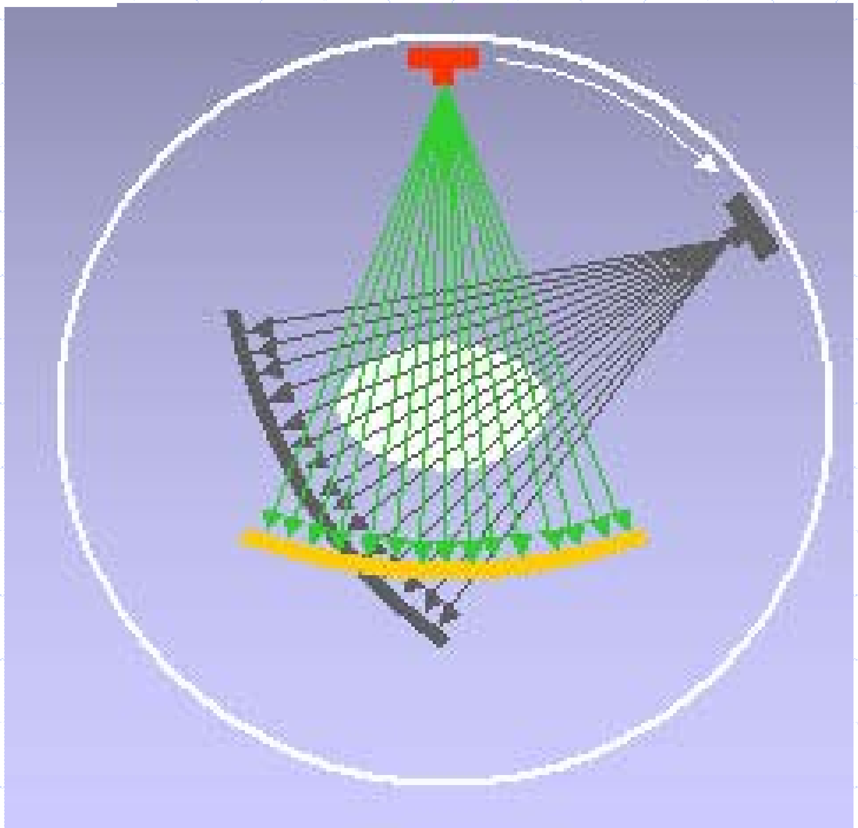

Fourth generation

- Stationary ring of detectors (600 – 4800 scintillators)
- Rotating X-ray source
- total scan time ~ seconds
- reconstruction time ~ seconds
- Slice thickness 1mm

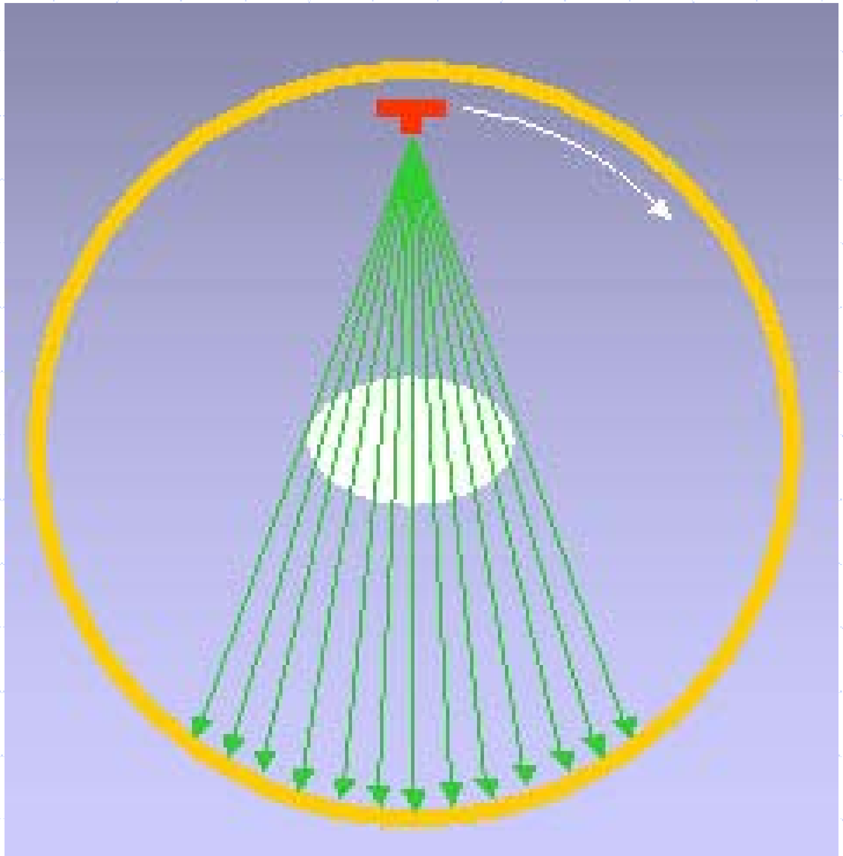

3D volumes constructed as a series of 2D slices

Fifth: electron beam scanner

Helical (sixth generation)

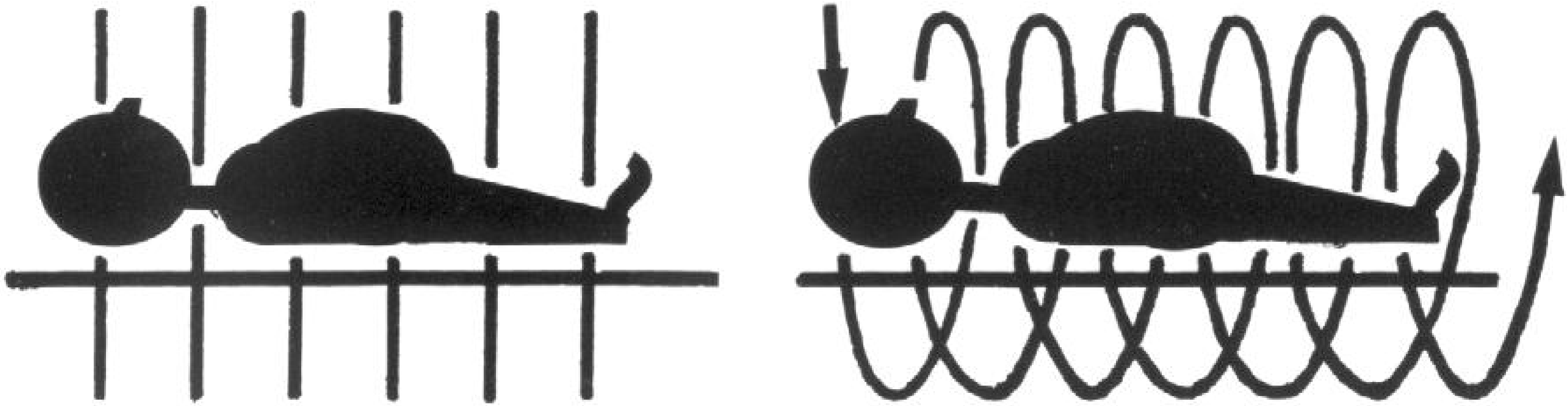

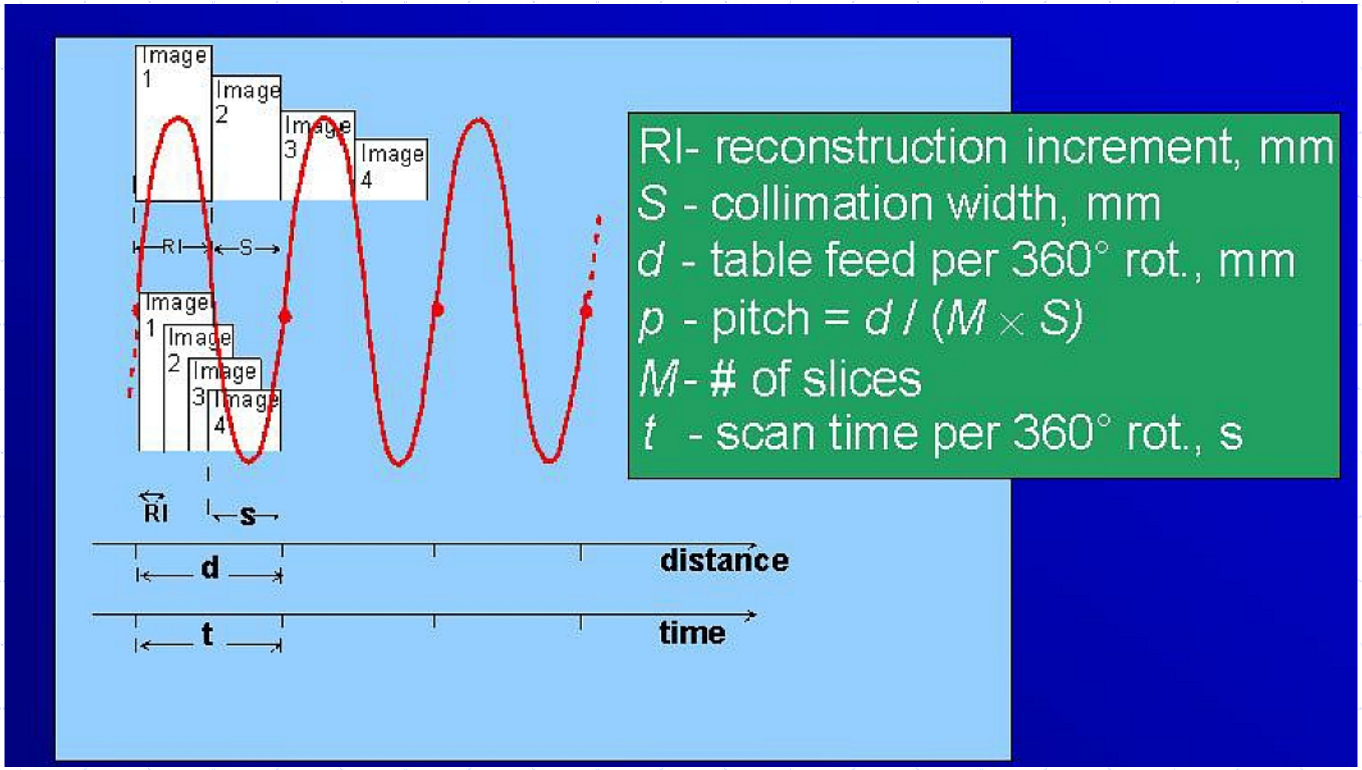

	Conventional CT	Helical CT
scanning	N 360° scans at positions z_1 to z_n	One scan of n-360° from positions z_1 to z_n
Pre-processing	corrections	corrections
intermediate		Z-interpolation
reconstruction	Convolution and backprojection	Convolution and backprojection
result	N images at positions z_1 to z_n	Images at arbitrary positions from z_1 to z_n

	1972	1980	1990	2000
Acq. time	300 s	5-10 s	1-2 s	0.3-1 s
Data 360°	57.6 kB	1 MB	2 MB	42 MB
Data helical	--	-	24-48 MB	200-500 MB
Matrix	80x80	256x56	512x512	512x512
Power	2 kW	10 kW	40 kW	60 kW
Slice thick.	13 mm	2-10 mm	1-10 mm	0.5-5 mm
Spatial res.	3 lp/mm	8-12 lp/mm	10-15 lp/mm	12-25 lp/mm
Contrast res	5 mm/5 HU 50 mGy	3 mm/3 HU 30 mGy	3 mm/3 HU 30 mGy	3 mm/3 HU 30 mGy

Status

3D medical CT:

- Helical trajectory
- Similar to 3rd generation CT but with multiple rows of detectors (4, 8, 16, 32, 64, now even up to 640 rows)
- FDK-like approximate reconstruction

3D lab-based CT:

- 3D cone-beam micro-CT using circular trajectory
- 512^2, 1024^2, 2048^2 (flat-panel – CCD – II detectors-...)
- FDK approximate reconstruction

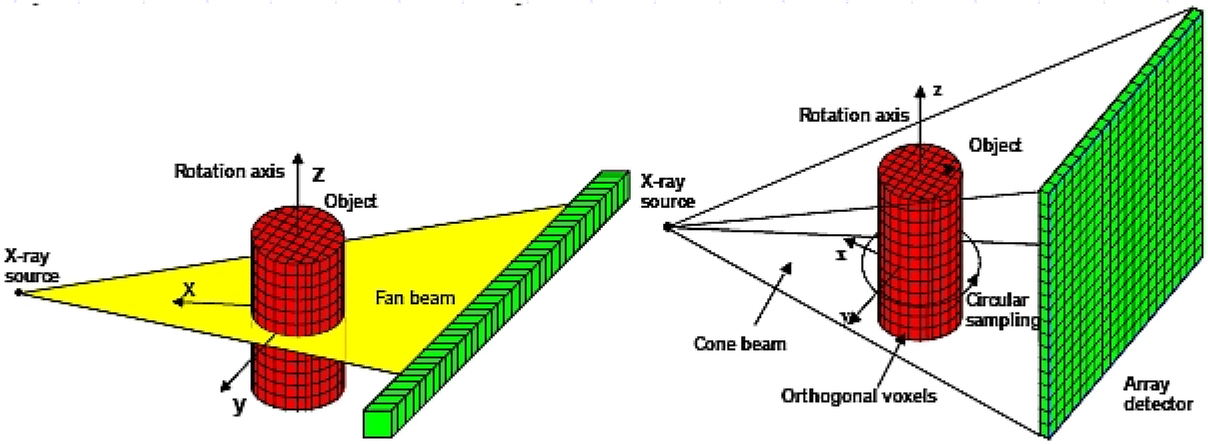

Design concepts

Detector
Screen: efficiency, spatial resolution
Pixel size: spatial resolution,signal, Fov
Dynamic range, daq time

Source
Energy
Current
Focal spot size
Focal spot stability

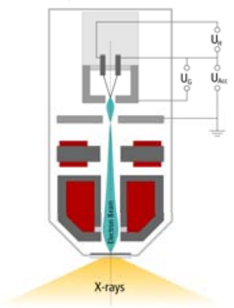

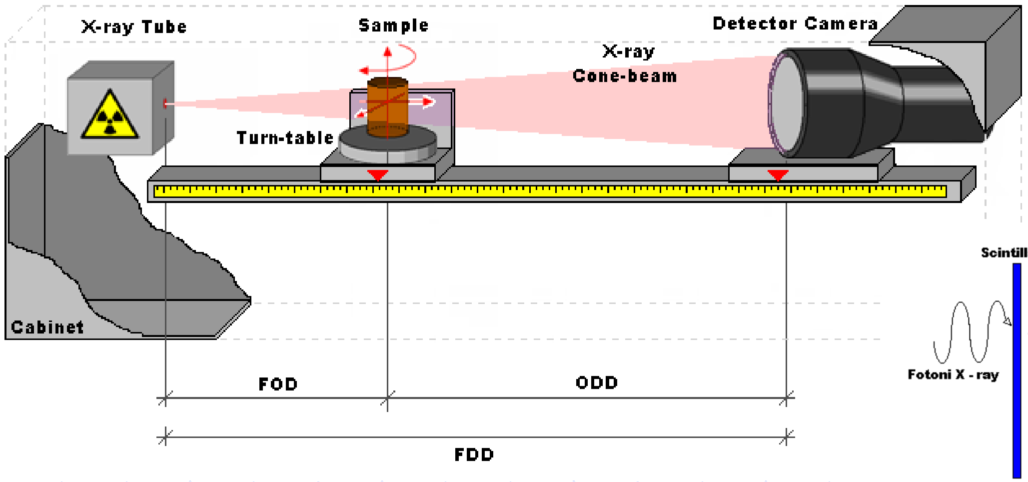

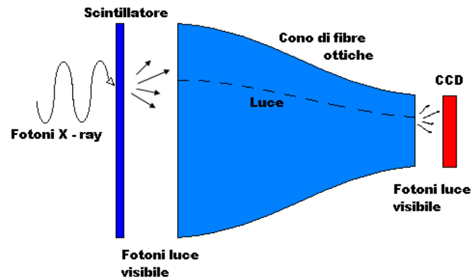

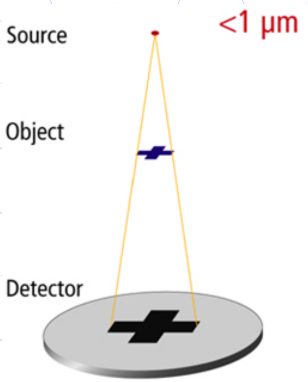

Magnification
x-ray flux
Penumbra
field of view

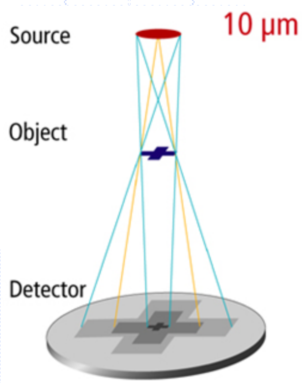

Source

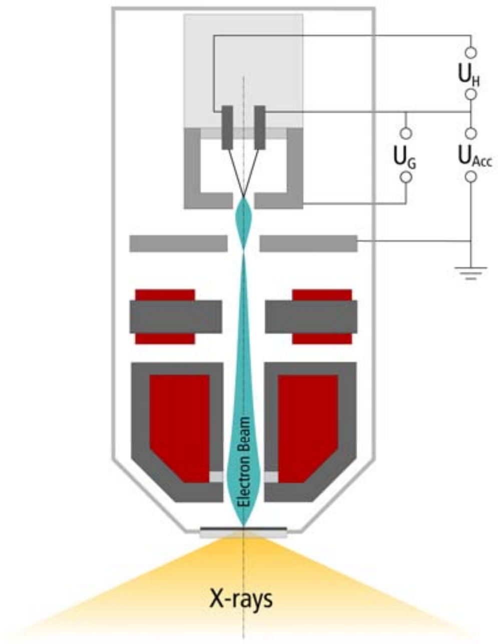

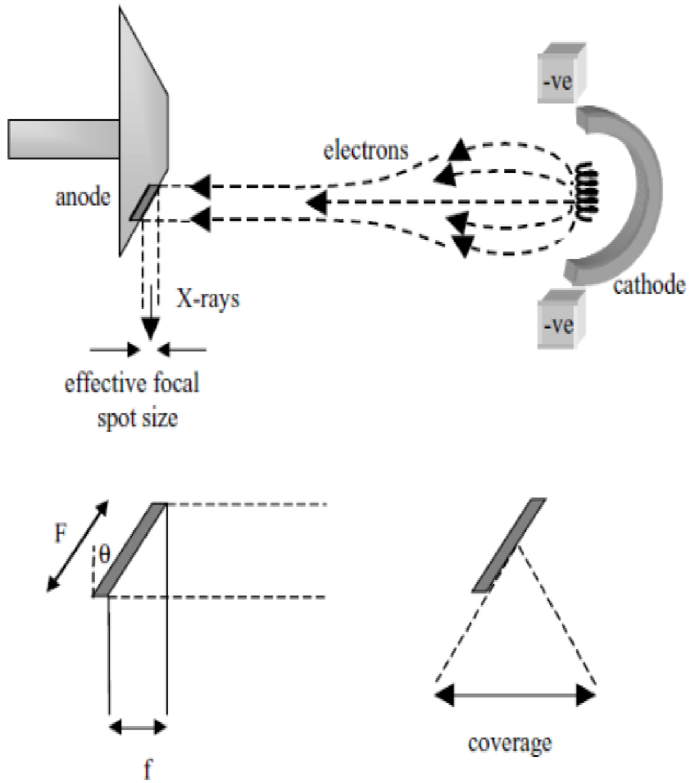

FIGURE 1.4. (Top) A negatively charged focusing cup within the X-ray cathode produces a tightly focused beam of electrons and increases the electron flux striking the tungsten anode. (Bottom) The effect of the anode bevel angle θ on the effective focal spot size f and the X-ray coverage.

Focal spot size
Emission angle
Material
Technology

$\theta \approx 5° - 20°$

Source

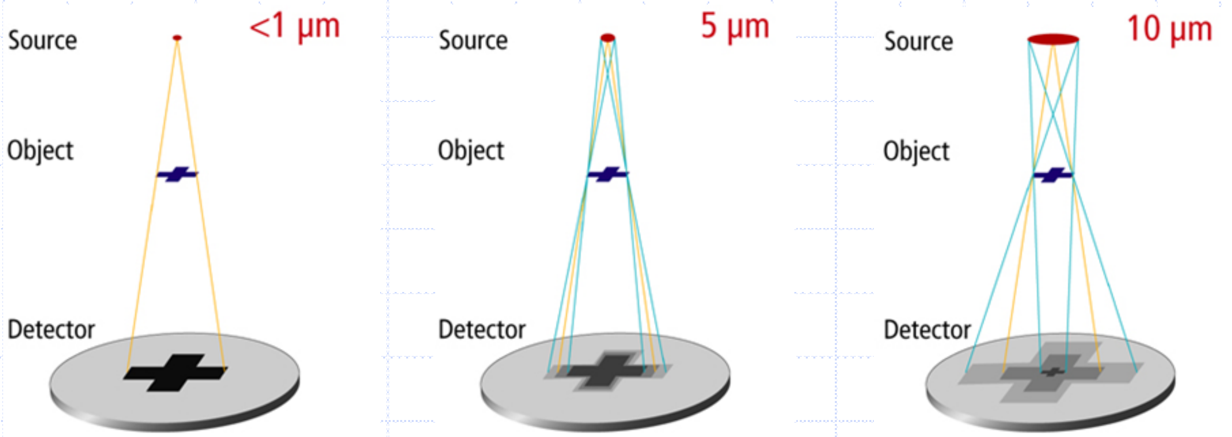

unsharpness $$U_{FS} = \frac{M-1}{M} FS$$

Heat dissipation
Stability
Phase effects

Source

100 kVp, θ = 15°, 0.2 mm Be window
500 mm air

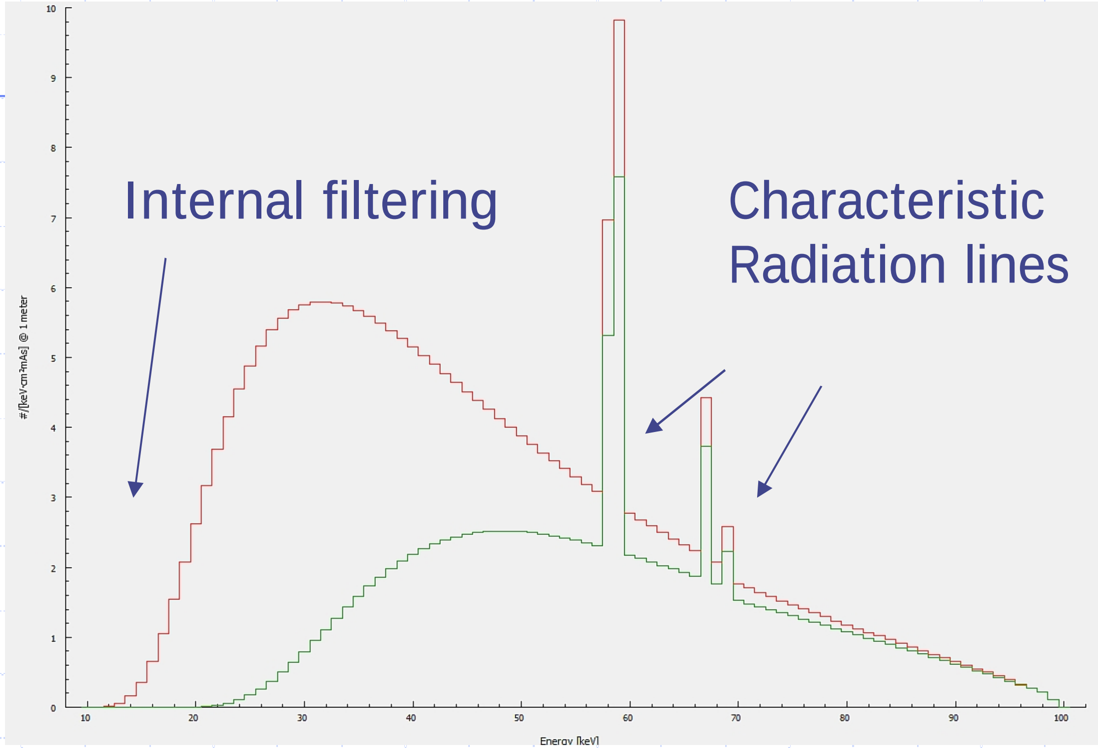

1.50 mm Al

Mean energy 46.2 keV

1st HVL 2.38 mm Al, 2nd HVL 4.20 mm Al, HVL1/HVL2 = 0.567

0.25 mm Cu

Mean energy 57.3 keV

1st HVL 6.46 mm Al, 2nd HVL 8.00 mm Al, HVL1/HVL2 = 0.807

Source

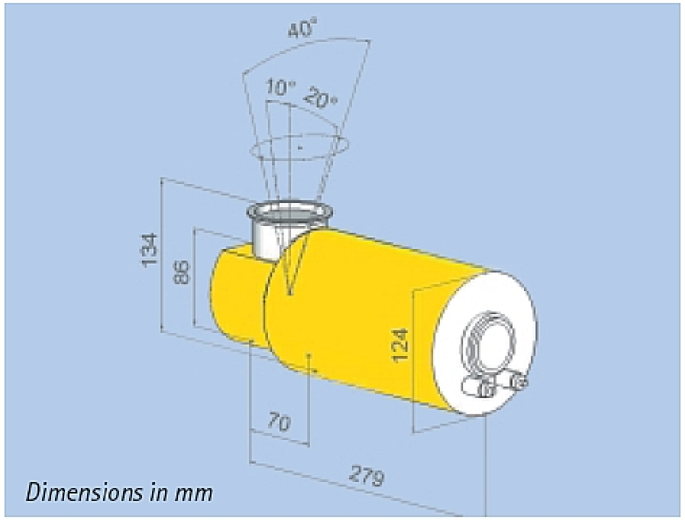

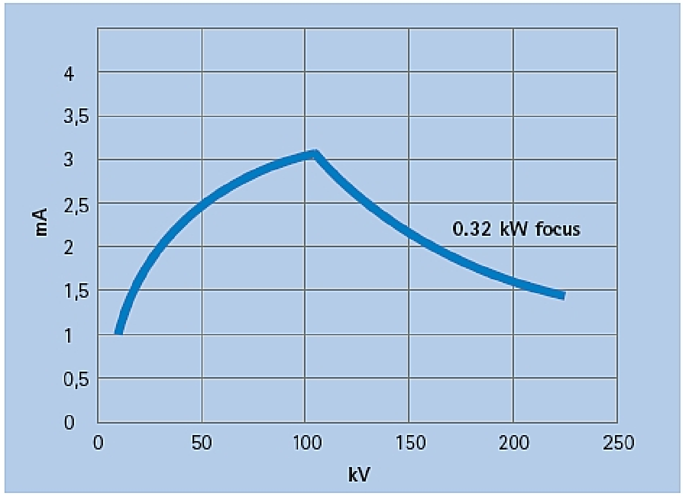

Loading data: shown are the max. permissible anode currents. Within the X-ray system these anode currents may be limited by power suppliers or generators.

Max. tube voltage	225 kV
Focal spot size	
(acc. EN12543)	0.5 mm
(acc. IEC336)	0.2
Max. power	
(small / large focus)	0.32 kW
Max. tube current at 225 kV	1.4 mA
Emergent beam angle	40 ° x 30 °
Inherent filtration[1]	0.8 mm Be + 4 mm Al
Leakage radiation[2]	< 5.0 mSv/h
Coolant	Water
Max. inlet temperature	45 °C
Min. flow rate	4 l/min
Enviromental Conditions	
Operation temperature	-10 °C...+40°C
Storage temperature	-25 °C...+70°C
Relative humidity	
- Operation	90 %
- Storage	95 %
Weight	11 kg
H.V. connection	Flange R12
Approval	PTB
Order No.	9421 172 31103

[1] Al-filter removable by using tools;
Al-filter acc. DIN 54113 and SSI FS1989:2

[2] Measured at 1.0 m distance from the focal spot with X-ray port closed and X-ray tube operating at full load.

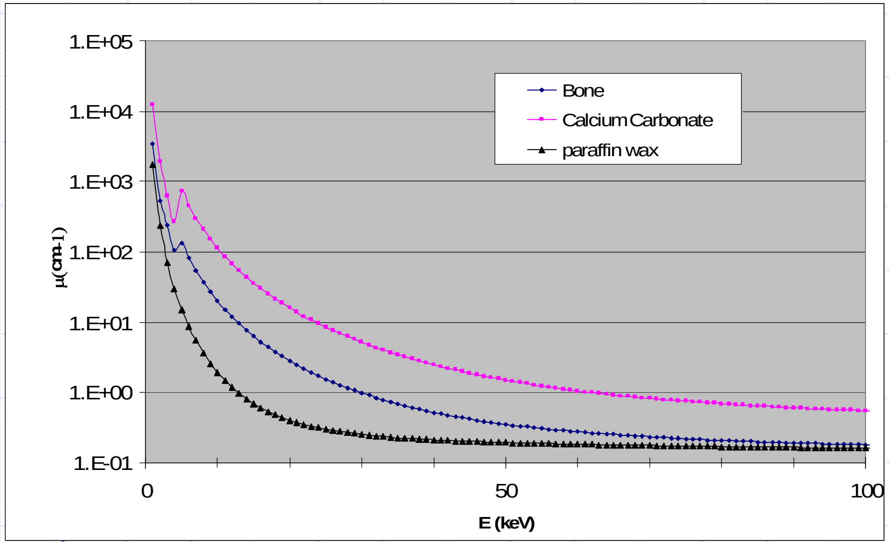

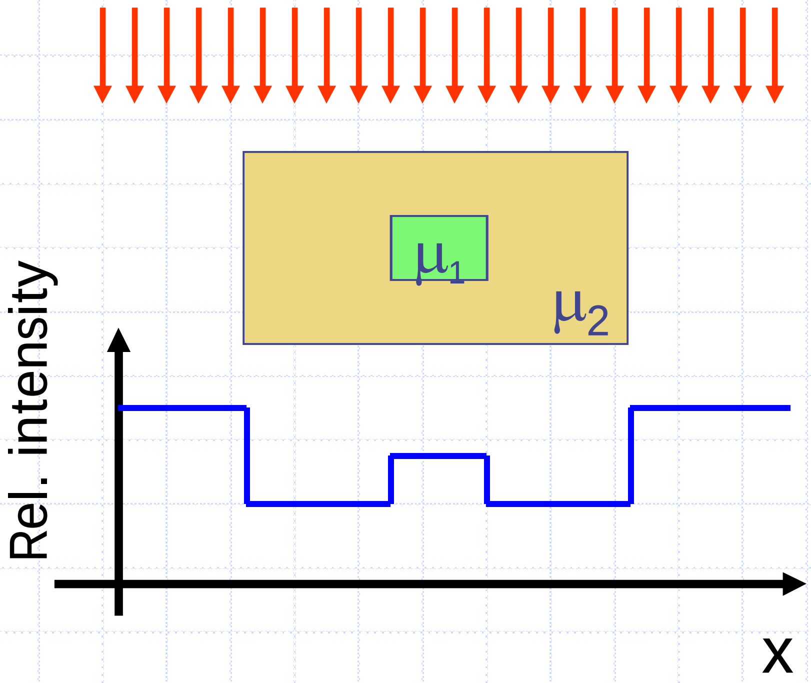

$$N_o = N_i e^{-\sum_k \mu_k \Delta x}$$

Lower energy

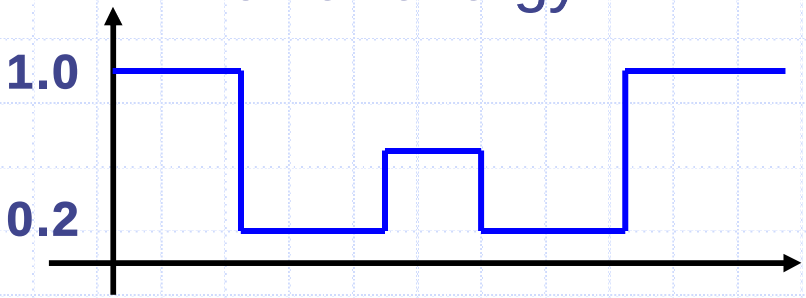

Higher energy

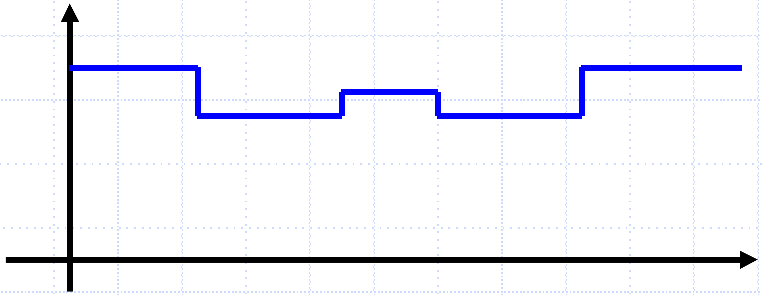

0.1 – 0.2 transmission > 5 σ_n

Detector

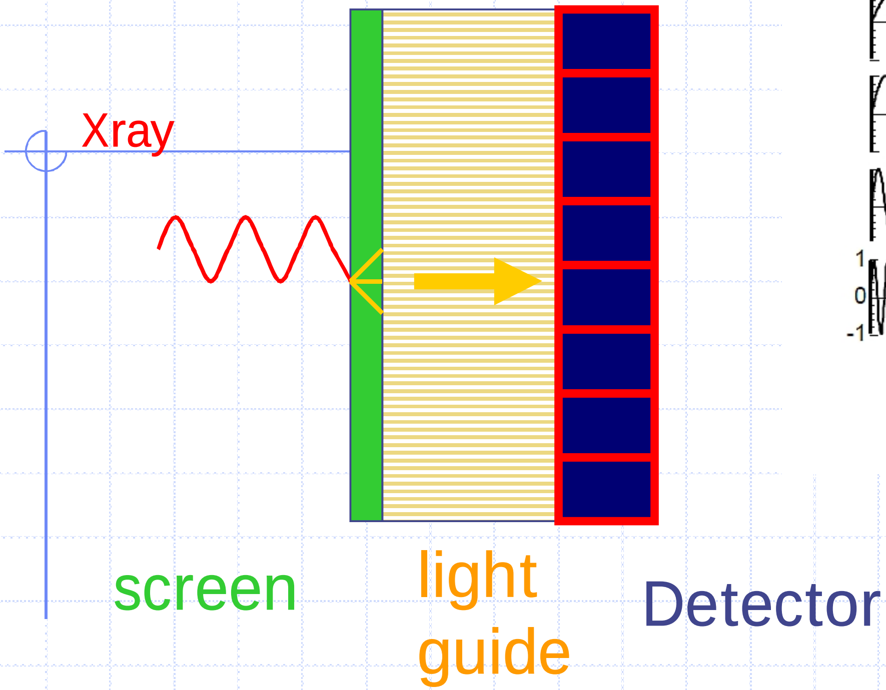

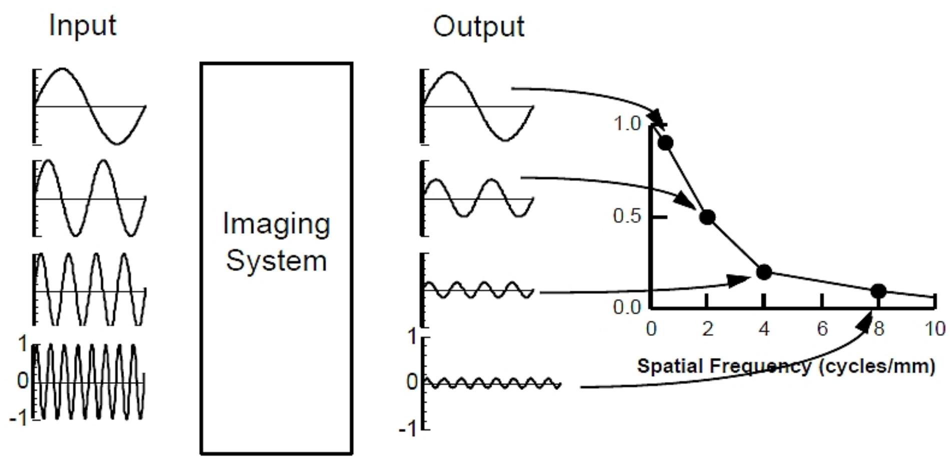

measures change in the amplitude of sine waves

Direct (aSe, Si)
Powders
Structured

Fov
High energy

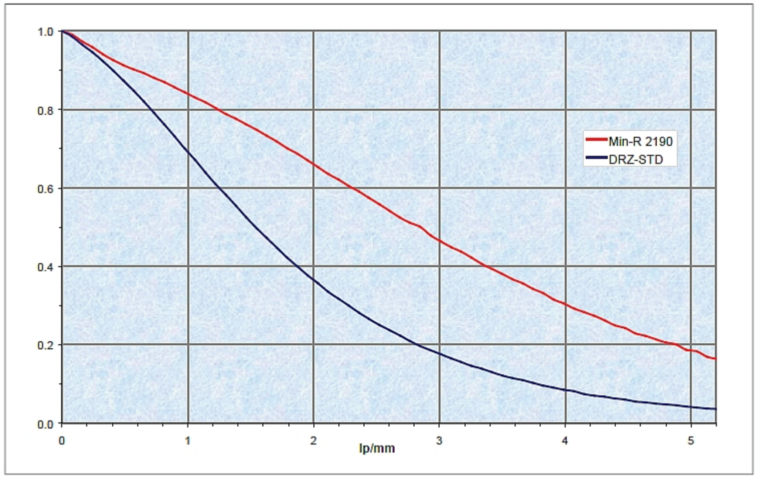

SkiaGraph Camera MTF

Scintillator	35kVp	50kVp
Min-R 2190	98 ADU/mR	105 ADU/mR
DRZ-Std	214 ADU/mR	257 ADU/mR

Detector

CCD Area, sCMOS

Flat Panel (large area CMOS)

GOS (+FOP)
CsI (+FOP)

Flat Panel (aSi/aSe) → Direct conversion

Photodiode array → CsI, Ceramic

Single photon counting → MediPix, Pixirad, ...

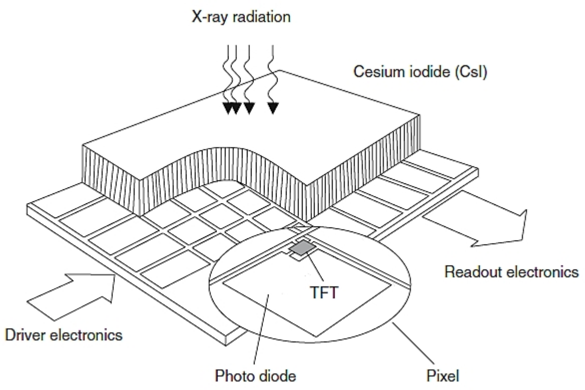

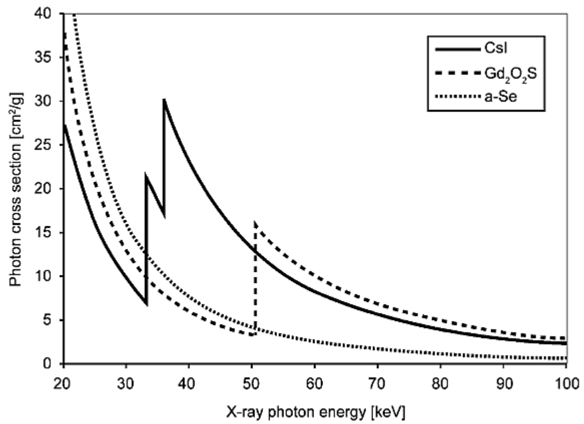

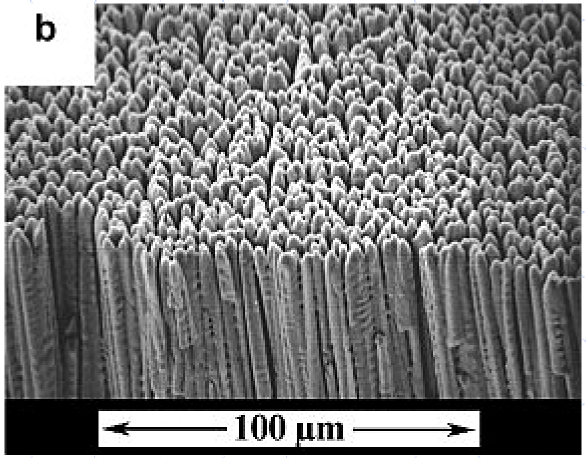

Detector

Specification	Minimum	Typical	Maximum	Units
Resolution	-	2000x2048	-	pixels
Active Area	-	192x197	-	mm
Avg. dark current (at 23°C)	-	40	-	ADU/sec
Read noise (rms, at 1 fps)	-	< 1	-	electrons
Dynamic range	-	72	-	dB
Conversion gain	-	1400	-	electrons/ADU
Frame rate	0.05	-	1.4	fps
Supply voltage	6.0	6.5	8.0	V
Supply current	-	> 30	-	%
Operating temperature	0	-	50	°C
Dimensions (LxWxH)	-	242x279x33	-	mm
Weight	-	3.5	-	kg

The [redacted] camera is capable of real-time imaging at up to 1.4 fps, 12-bit digital contrast resolution, 5 lp/mm spatial resolution and features a choice of scintillators providing impressive

Dynamic range 72 db ~ 4000:1 -> 12 bit

Detector

			fps	
	Matrix	Pixel (μm²)	AO	AP
Square	1024 × 1024	200 × 200	15	25
	512 × 512	400 × 400	30	50

Lag	< 8% 1st frame
Dynamic Range	> 78 dB (AO), > 88 dB (AP)
Energy	20 keV – 15 MeV

LAG: not suitable for CT!

Pixel Size	74.8 μm	74.8 μm	74.8 μm
Sensitive Area	114.9 x 64.6 mm	145.4 x 114.9 mm	290.8 x 229.8 mm
Resolution	1536 x 864 px	1944 x 1536 px	3888 x 3072 px
Sensor Type	CMOS active pixel sensor	CMOS active pixel sensor	CMOS active pixel sensor

Max Frame Rate (fps)

	1207NDT		1512NDT			2923NDT	
Pixel Binning	Camera Link	GigE Vision	Camera Link	GigE Vision	USB	Camera Link	GigE Vision
1x1	60	24	26	11	6	26	3
1x2	119	52	53	23	13	53	6
1x4	163	105	72	46	8	72	11

Reconstruction

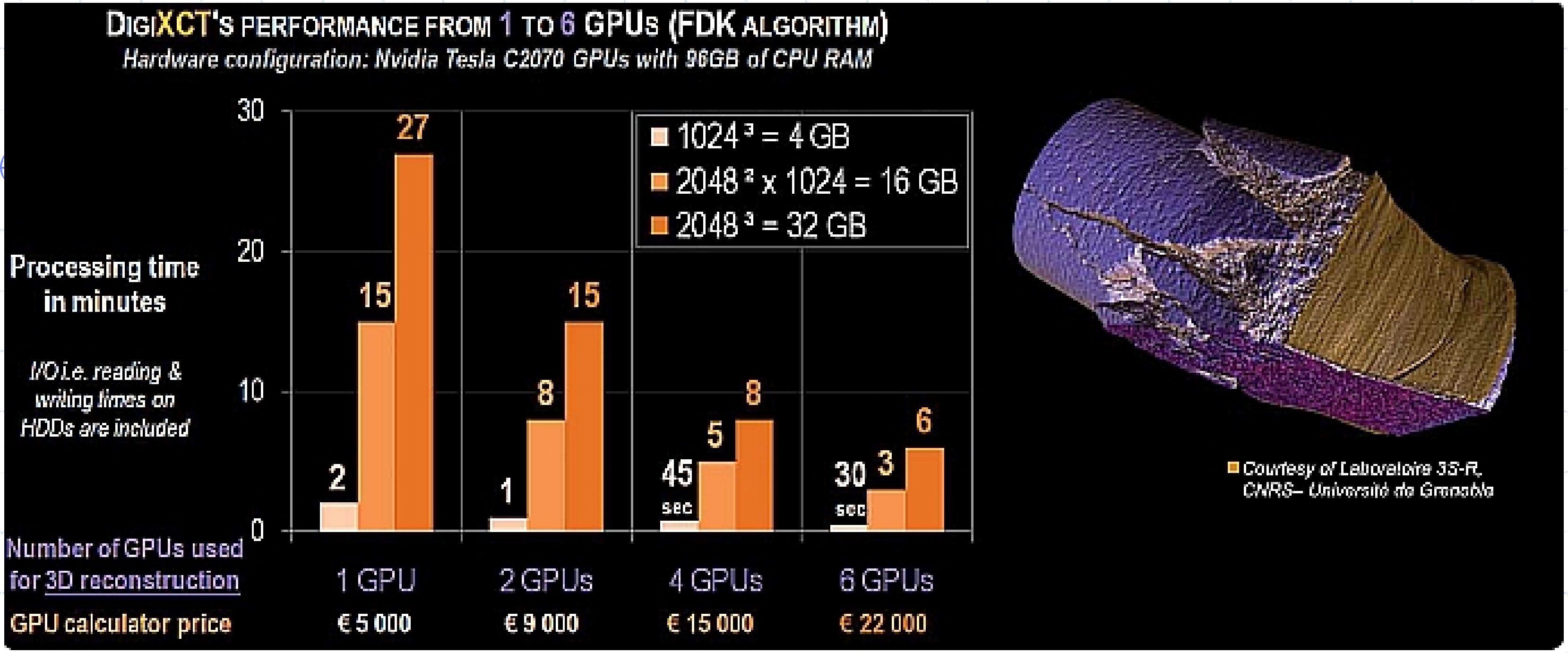

Volume 150 x 150 x 150 mm^3

Isotropic voxel size 50 µm

dataset = 3000^3 x 4 = 108 GB

Isotropic voxel size 60 µm

dataset = 2500^3 x 4 = 62.5 GB

DATA I/O / PROCESSING / STORAGE

Reconstruction

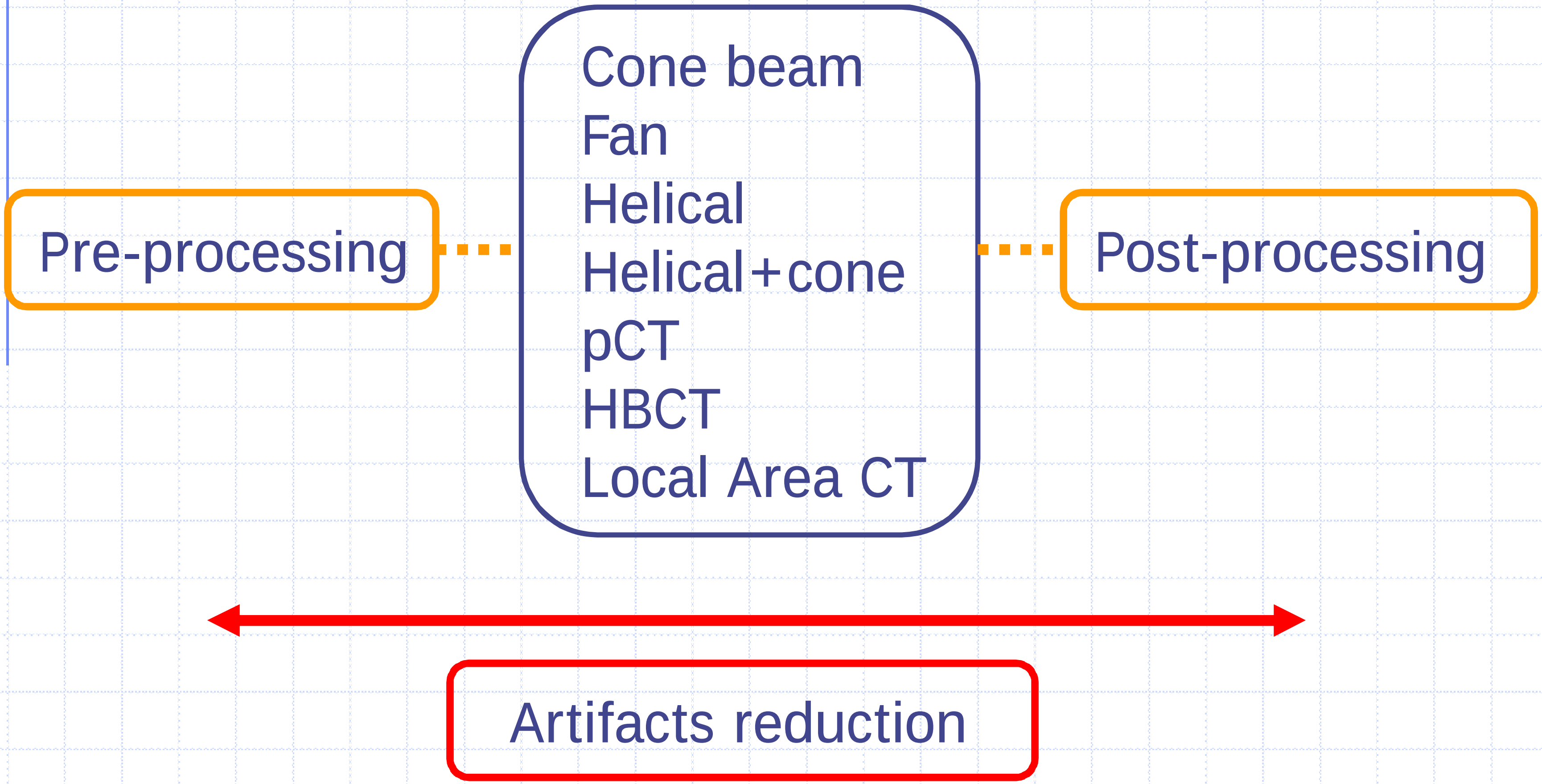

Geometry

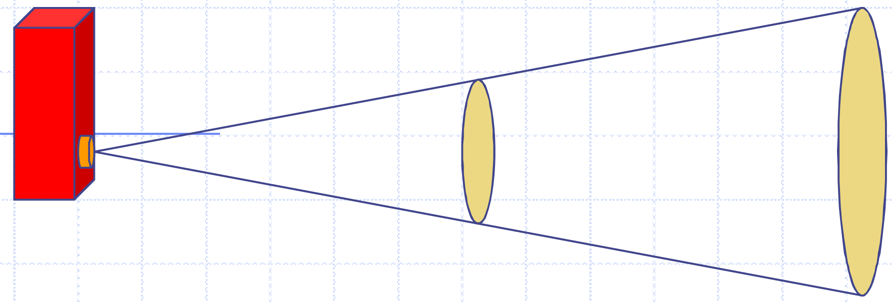

Intensity~1/d²

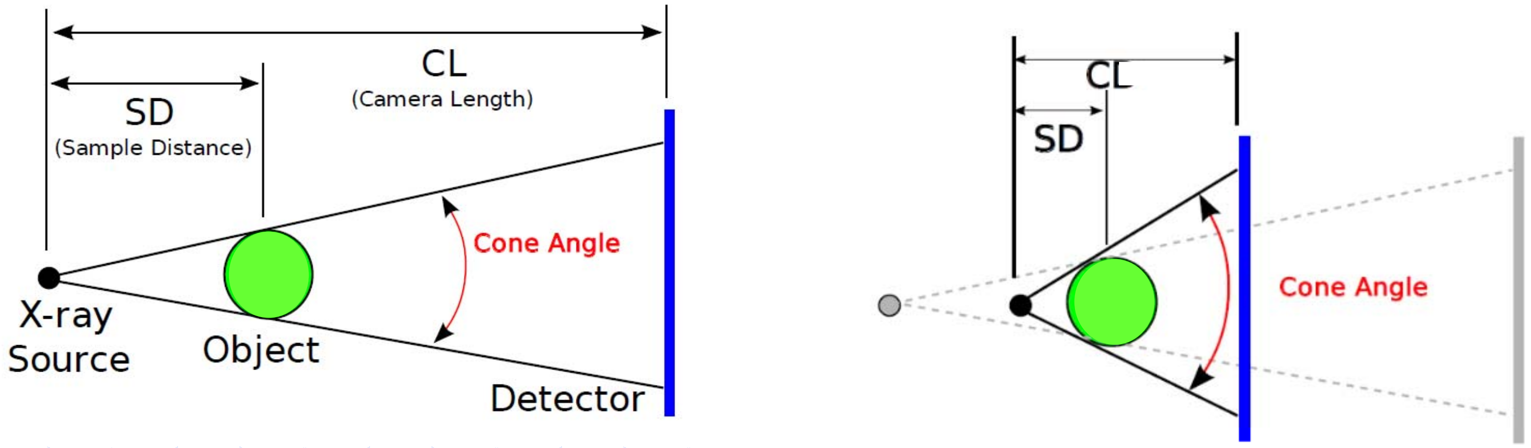

FDK filtered back-projection is reasonable up to ~10°

With microfocus sources phase contrast imaging possible

Unsharpness

Pixel Size $$U_{PS} = \frac{2}{M} PS$$

Focal spot $$U_{FS} = \frac{M-1}{M} FS$$

$$U_{TOT} = \sqrt{U_{FS}^2 + U_{PS}^2}$$

ASTM E 2698

$$U_{TOT} = \frac{1}{M} \sqrt[3]{(M-1)^3 FS^3 + (1.6PS)^3}$$

Examples

FS = 8 μm, PS = 25 μm, M =5

U_{TOT} = 9.2 μm PS_{eq} = 5 μm

FS = 16 μm, PS = 50 μm, M =1.25

U_{TOT} = 64 μm PS_{eq} = 40 μm

Number of projections

Spatial and angular sampling on Fourier space

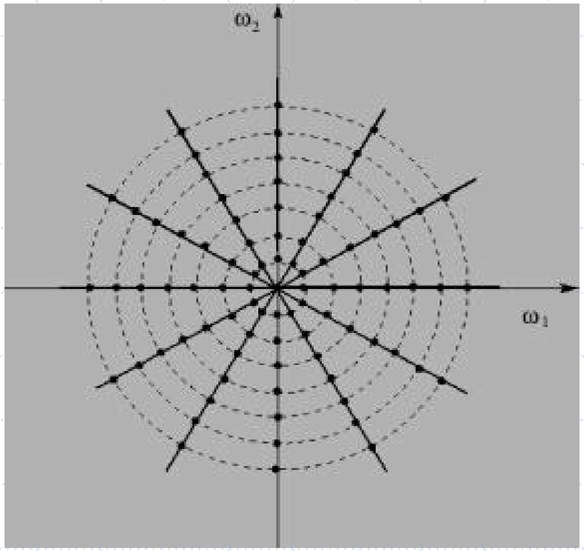

$K \approx \pi / 2\ N$

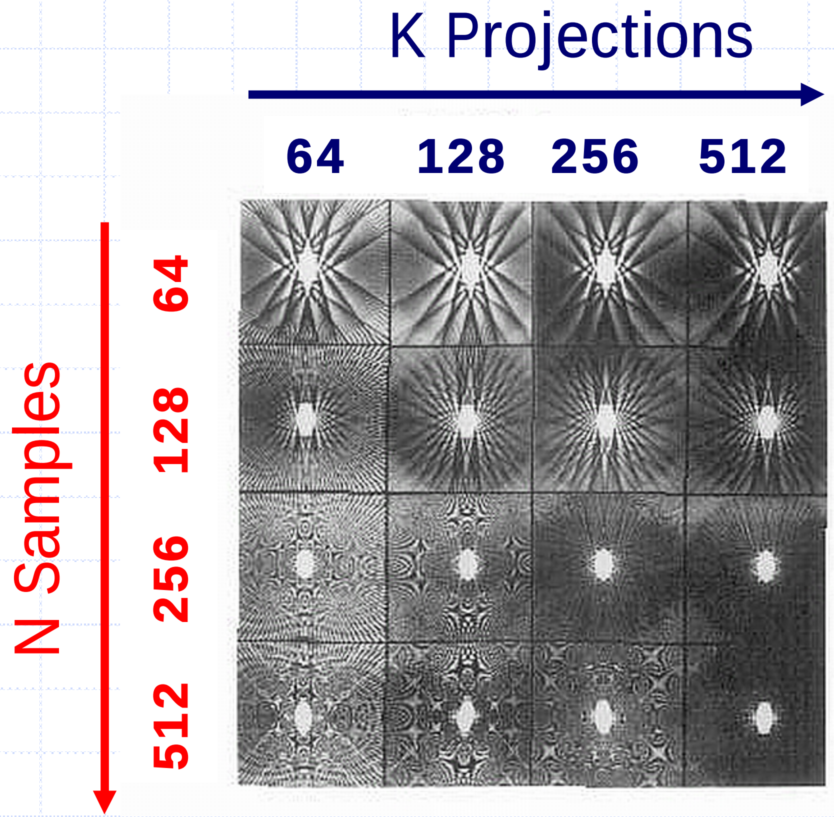

Reconstruction of an ellipse

σ_{pn} pixel noise (standard deviation evaluated on 2D slices)

$$\sigma_{pn} = \frac{\kappa \cdot \pi}{PS \cdot \sqrt{Np}} \cdot \frac{1}{\sqrt{I \cdot t \cdot Na}}$$

k = constant dependend on rec algorithm
(smooth kernel reduces noise, but also spatial resolution)
PS = pixel size (mm^2)
Np = number of projections
I = source current (mA)
t = integration time of the detector (s)
Na = image averaging number

Artifacts

Sample
1- motion
2- metallic materials
3- dimension > scan field

Scanner
1- rings
2- geometry
3- stability

Physics
1- Beam Hardening
Cupping & Streaks
2- Undersampling
3- Photon starvation
4- Partial Volume

Technique
1- helical in transverse plane
2- helical in multislice
3- multiplanar and 3D reconstrucion
4- cone beam effect

Artifacts simulation

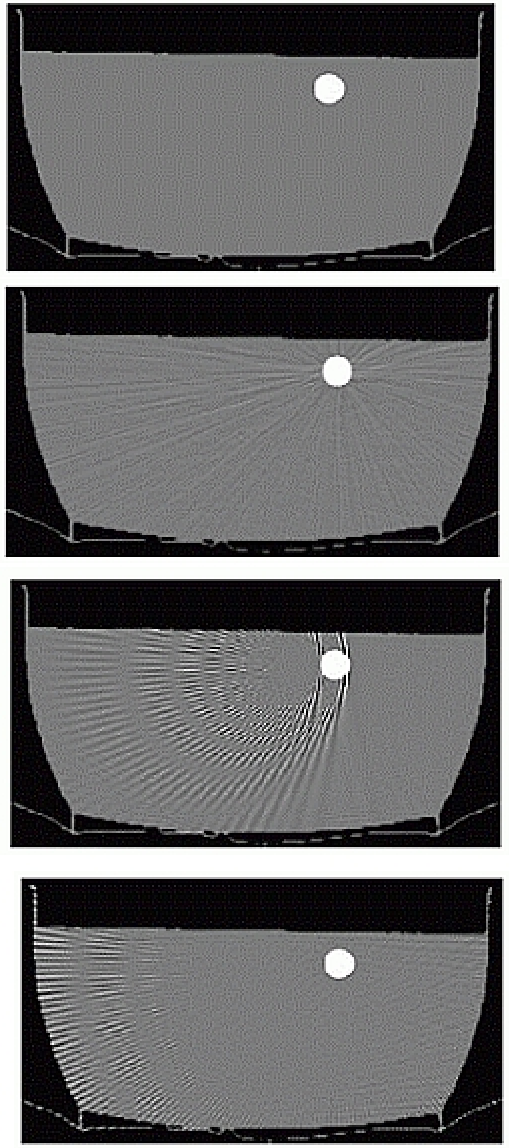

- Normal phantom (simulated water with iron rod)
- Adding noise to sinogram gives rise to streaks
- Aliasing artifacts when the number of samples is too small (ringing at sharp edges)
- Aliasing artifacts when the number of views is too small

Artifacts simulation

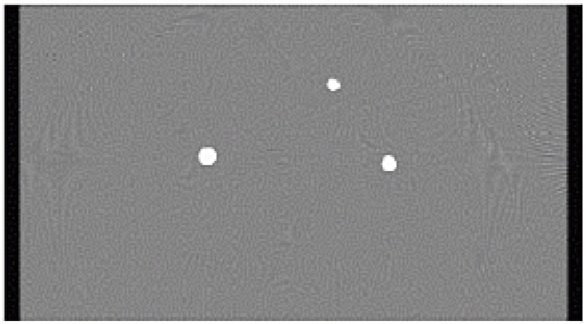

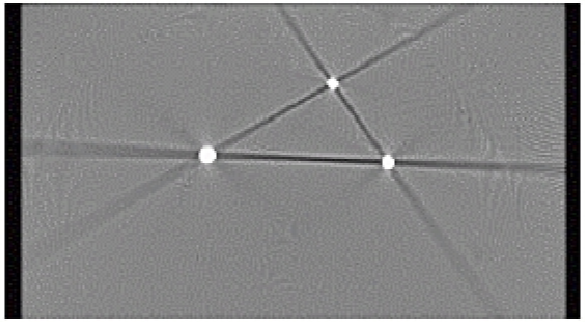

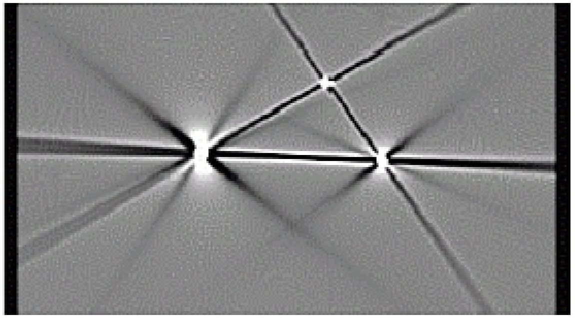

- Normal phantom (plexiglas plate with three amalgam fillings)
- Beam hardening artifacts
  - non-linearities in the polychromatic beam attenuation (high opacities absorb too many low-energy photons and the high energy photons won't absorb)
  - attenuation is under-estimated
- Scatter (attenuation of beam is under-estimated)
  - the larger the attenuation, the higher the percentage of scatter

Artifacts simulation

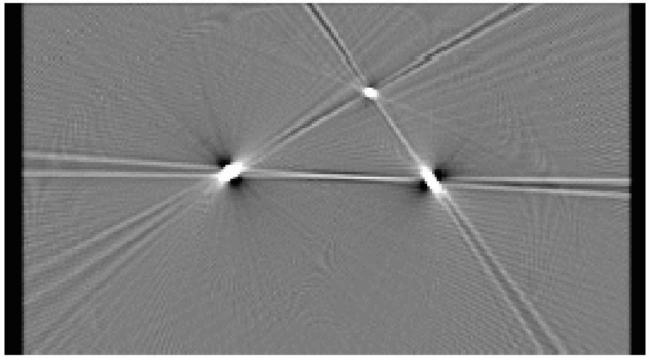

single pixel traversed
by individual rays:

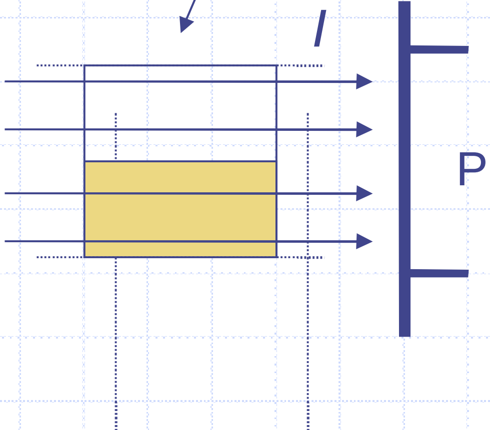

•will underestimate the attenuation

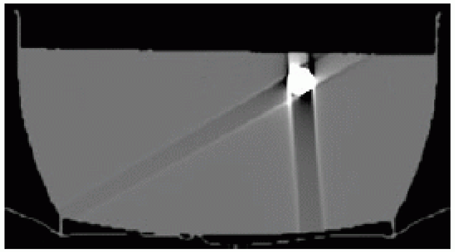

Motion artifacts
rod moved during acquisition

More realistic cases

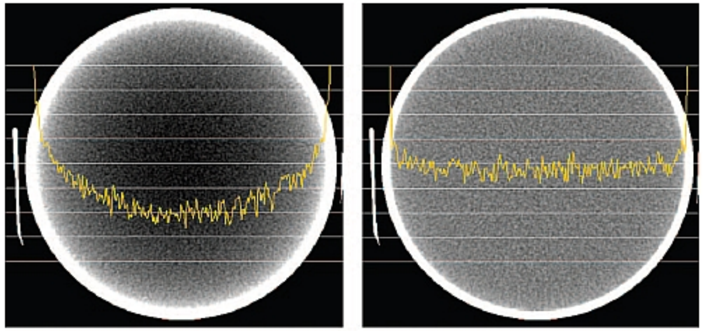

a. b.

Figure 3. CT number profiles obtained across the center of a uniform water phantom without calibration correction **(a)** and with calibration correction **(b)**.

Beam hardening: cupping

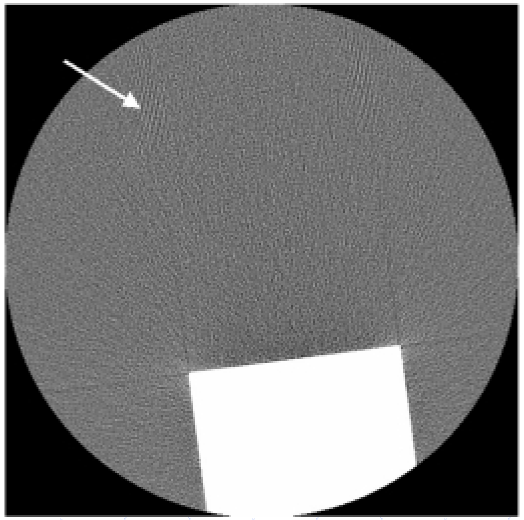

Undersampling

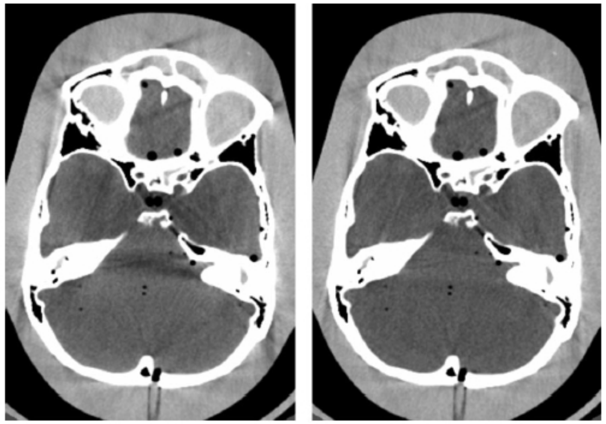

a. b.

Figure 6. CT images of the posterior fossa show the dark banding that occurs between dense objects when only calibration correction is applied **(a)** and the reduction in artifacts when iterative beam hardening correction is also applied **(b)**. (Reprinted, with permission, from reference 1.)

Beam hardening: streaks

Figure 9. CT image of a shoulder phantom shows streaking artifacts caused by photon starvation.

Photon starvation

More realistic cases

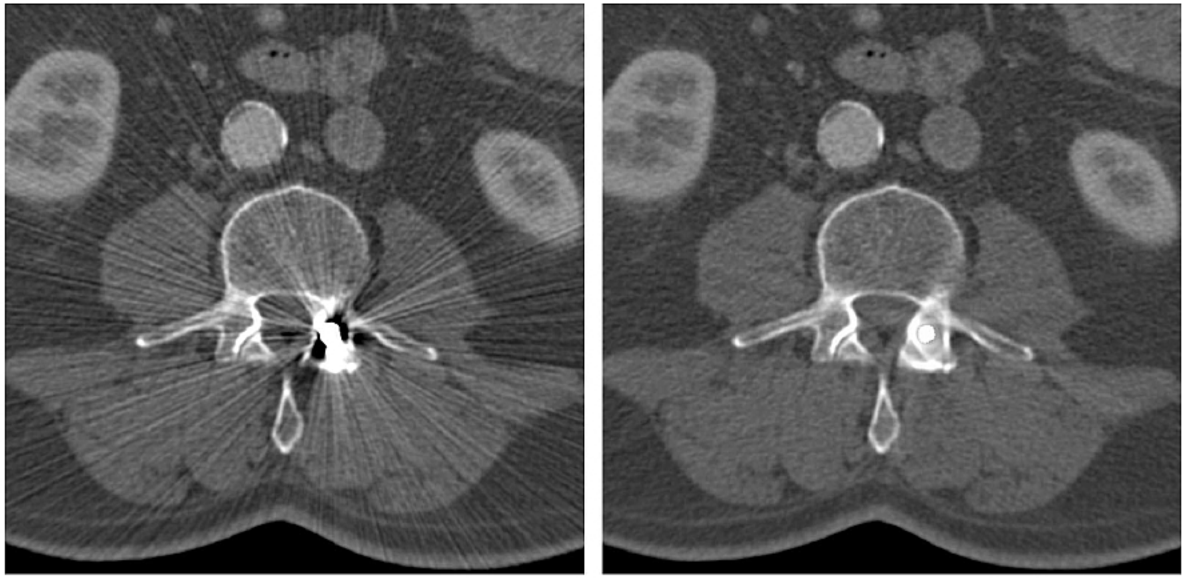

a. b.

Figure 15. CT images of a patient with metal spine implants, reconstructed without any correction (**a**) and with metal artifact reduction (**b**). (Courtesy of Siemens, Forchheim, Germany.)

Metal artifacts

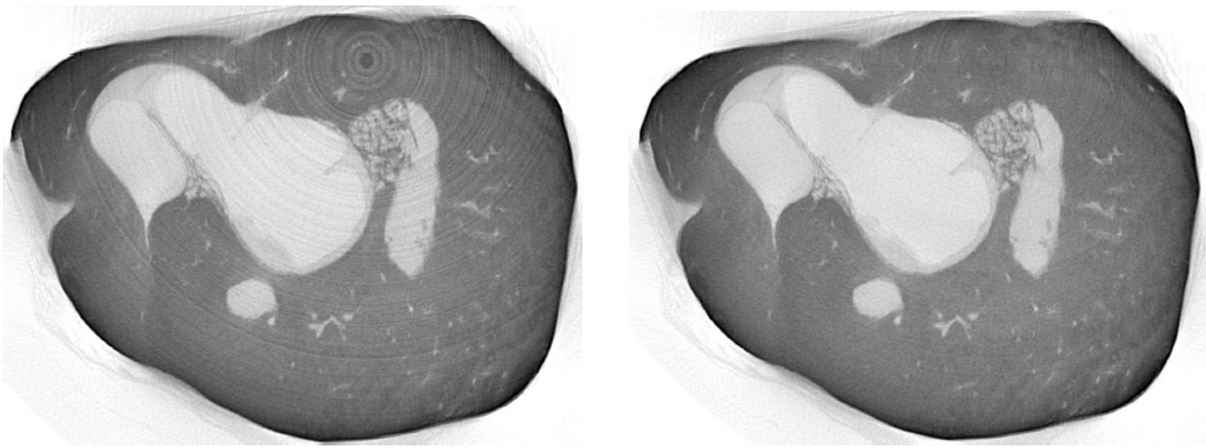

Rings

More realistic cases

Figure 18. CT image of the body obtained with the patient's arms down but outside the scanning field shows streaking artifacts.

Dimensions > FOV

Imaging Requirements

Something to know:

1. The size of the object you want to scan
2. The material the object is made of
3. The level of fine detail or density differences you want to see
4. How fast you want to see the results
5. Where you want to place the instrument
6. Who will use it

New high-speed Computed Tomography system for 3D mass production process control

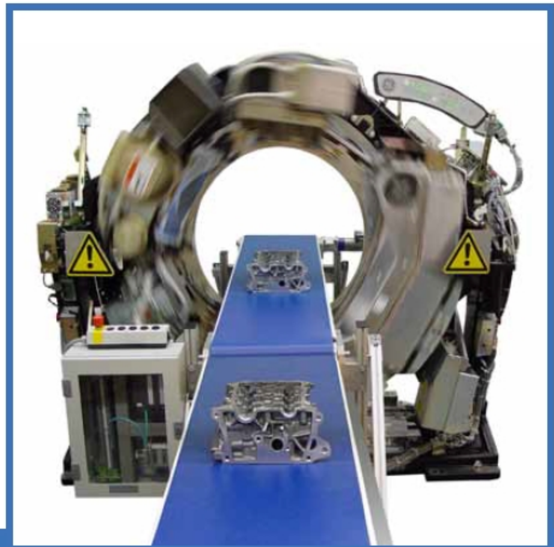

Continous CT helix scan

RayScan Mobile can be applied to the tomographic inspection of pipelines, airplane wings, rotor blades, pillars or statues. The modular design permits to optimise RayScan Mobile for each particular application.

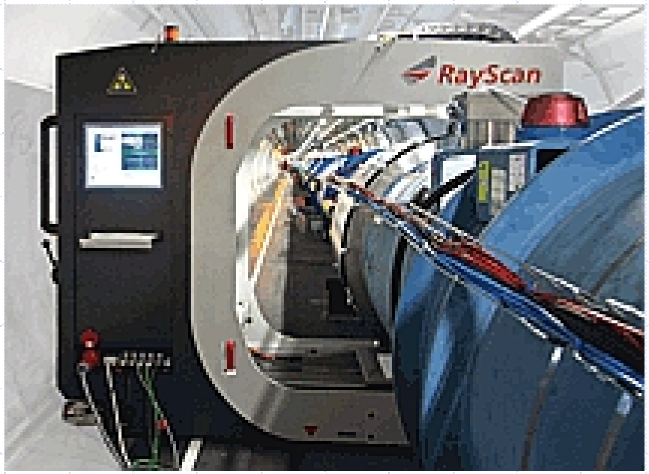

Volume CT of Large Objects

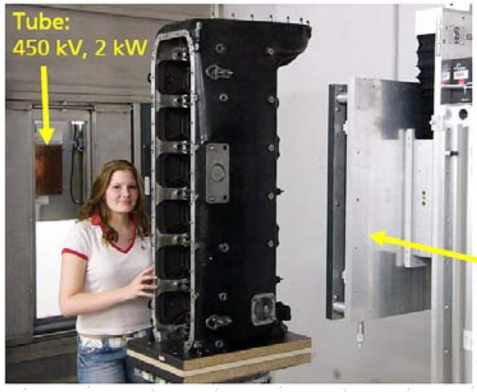

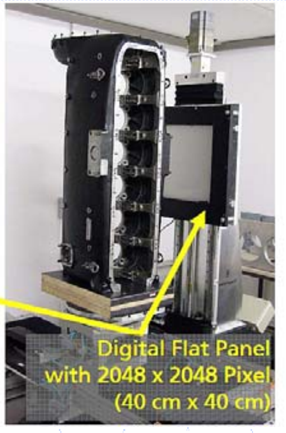

Workpeice Dimensions	
Maximum Scan Diameter	35 mm – 75 mm
Maximum Scan Height	25 mm – 45 mm
Detector	
Number of Pixels	1 Megapixel – 3 Megapixel
Pixel Size	20µm - 75µm
AD Conversion	16 Bit
X-Ray Source	
Max Acceleration Voltage	80 kV – 130 kV
Power	10 W – 90 W
Cooling	Air Integrated
Mechanics	
Linear Guide Ways	Granite based with high precision linear guideways
Turntable Bearings	Roller Bearing or Air Bearing
Position Measuring System	High-resolution optical precision measuring systems
Voxel Resolution	5µm - 40µm
Calibration & Monitoring	VDI / VDE 2630 (Draft)
Radiation Protection	Full radiation protection chamber
Set Up	Table Top Installation
Maintenance Access	Front

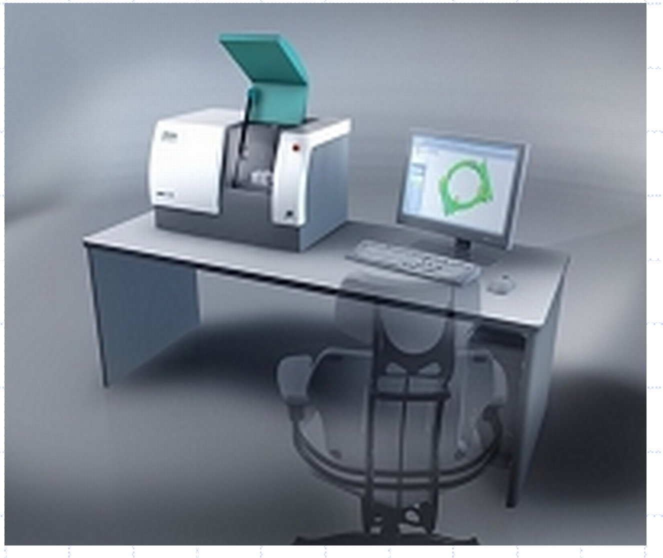

See you tomorrow at Mlab

Metal Oxide Semiconductor (MOS) Capacitor

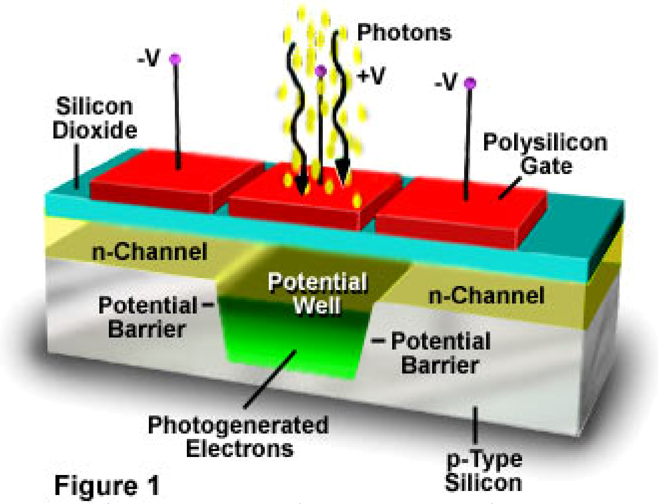

Figure 1

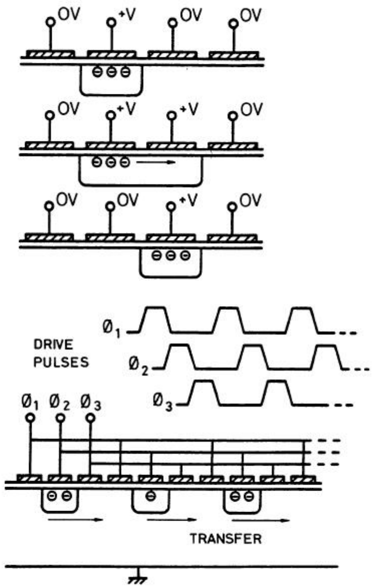

Figure 2a The charge-transfer mechanism employed in three-phase CCDs.

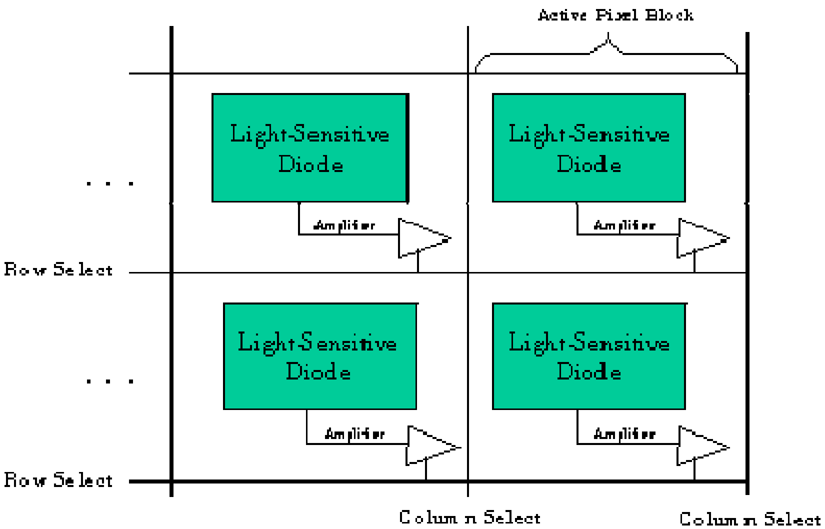

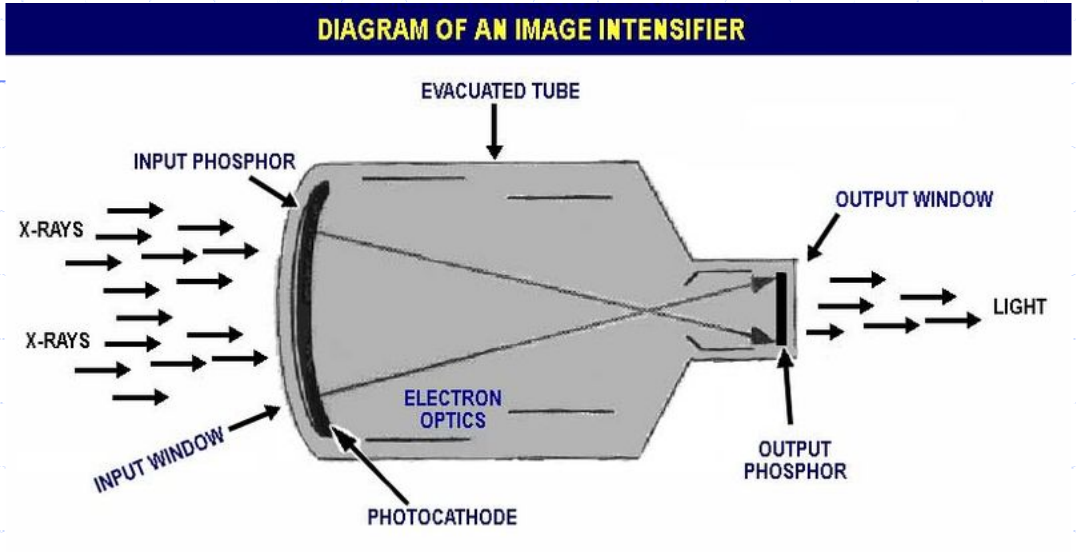

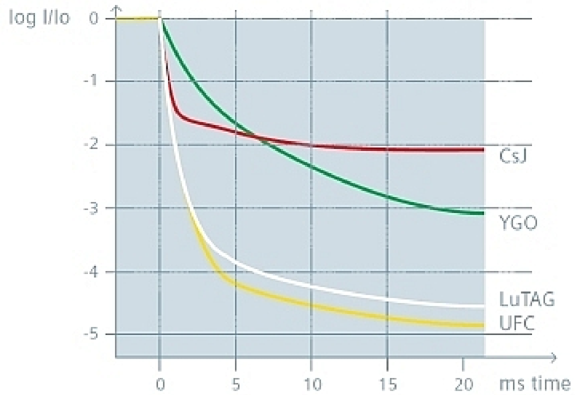

CsJ: Cesium Iodide
YGO: Yttrium Gadolinium Oxide
UFC: Siemens Ultra Fast Ceramic
LuTAG: Lutetium Terbium Aluminium Garnet